Volcanism and Sedimentation: New Insight into Arc-Related Volcanism and Sediment Deposition in a Synkinematic Paleoproterozoic Basin: Rosebel Gold Mine, Northeastern Suriname

Thomas Watson

A Thesis submitted to the faculty of the University of North Carolina at Chapel Hill in partial fulfillment of the requirements for the degree of Master of Science in the Department of Geological Sciences.

Chapel Hill
2008

Approved by

Dennis LaPoint

Kevin Stewart

Drew Coleman

Abstract

Thomas Watson: Volcanism and Sedimentation: New Insight into Arc-Related Volcanism and Sediment Deposition in a Synkinematic Paleoproterozoic Basin: Rosebel Gold Mine, Northeastern Suriname
(Under the direction of Dennis LaPoint, Kevin Stewart, Drew Coleman)

The recognition of a Paleoproterozoic island arc system, and associated depositional environments, preserved in the rocks of northeastern Suriname, relies on field, geochemical, and petrographic evidence obtained during this study, through the Rosebel Gold Mine (RGM). Geochemical and petrographic analyses of igneous rocks from RGM indicate that they are island arc related. Analyses of sedimentary rocks reveal the presence of four depositional environments, and different sediment provenances, reflecting different styles of deposition, and erosion of different source rocks. Structural analyses of the rocks at RGM have lead to the recognition of three phases of deformation: (D_1-D_3), resulting in thrusting and nappe style folding, steepening of these folds and development of pervasive axial planar foliation, and later, sinistral strike-slip faulting. These studies combined are used to generate a model of the evolution of the rocks at RGM during the Transamazonian orogeny.

To my Parents

ACKNOWLEDGEMENTS

I sincerely thank Dennis LaPoint for his encouragement during this project, and for sparking my interest in greenstone belts. I also thank Kevin Stewart and Drew Coleman for their guidance and encouragement. Additionally, I thank the geologists at the Rosebel gold mine, and the Surinamese and expatriate students for their support and help with some of the field aspects of this project.

Table of Contents

LIST OF TABLES

LIST OF FIGURES

I. Introduction:

The Rosebel Gold Mine (RGM), in northeastern Suriname, is set in Paleoproterozoic volcanic and sedimentary rocks that compose part of the Marowijne Supergroup. The Marowijne Supergroup locally consists of a basal-volcanic sequence interlayered with thin-sedimentary units (Paramaka Group), overlain by the mainly sedimentary Armina and Rosebel Formations (Voicu et al., 2001). The rocks of the Marowijne supergroup are metamorphosed to low-to-mid greenschist facies, and are locally cut by gold bearing quartz veins, that comprise the main source of ore for RGM.

The nature of the volcanic and sedimentary rocks that comprise the Paramaka group, the Armina and Rosebel Formations, and the nature of the contacts between these units have been subject to considerable debate (e.g. Bosma and Groeneweg, 1969, Gibbs and Barron, 1993). However, geological studies that might elucidate some of these uncertainties in Suriname have historically been hindered by political instability, tropical vegetation, and a thick tropical weathering profile. Recent mining and exploration of the RGM area have generated a significant amount of geological data, which is used in this paper to shed light on various aspects of the rock formations mentioned above. Field mapping, diamond drilling, aerial and ground magnetic surveys, and other mining-related activities have created a large database for potential use in assembling an understanding of the local geology.

This study incorporates some of the available data from RGM, supplemented with additional studies and analyses by the author, in an attempt to elucidate some aspects of Paleoproterozoic volcanism, sedimentation, and tectonism, in this part of the Guiana shield. Provenance studies of sedimentary rocks are used to determine the likely tectonic settings and environments of deposition (e.g. Dickinson et al., 1983). Whole-rock and trace-element-geochemical analyses of volcanic rocks are used to determine their likely tectonic provenances (e.g. Woodhead et al., 1992, Pearce and Peate, 1995, Hawkesworth et al., 1983, Wood, 1980) and oceanic vs. continental affinities (e.g. Barrett and MacLean, 1993). These studies, combined with detailed field and stratigraphic mapping, are used to generate a regional model of volcanism and sedimentation at RGM, associated with the Transamazonian orogeny.

II. Geologic Background:

II A. Lithofacies associations:

In general, the stratigraphy of greenstone belts is highly convoluted due to multiple episodes of deformation including folding and faulting. The structural complexity, in addition to intrinsically complex facies relationships of sedimentary units in greenstone belts can make stratigraphic interpretations a challenging task. Many studies of the 'stratigraphy' of greenstone belts have assumed that thick successions of metasedimentary and metavolcanic rocks occur without structural repetition, and that they have undergone relatively little deformation (Kusky and Vearncombe, 1997). However, as the understanding of greenstone belt geometry has increased greatly within the geologic community over the past several decades, the importance of detailed structural mapping in relation to understanding the stratigraphy becomes apparent. In many cases, complete re-appraisal of lithostratigraphic succession is required (Eriksson et al., 1994). The best approach is to classify stratigraphic successions based on genetic processes rather than specific rock types (Eriksson et al., 1994).

In this approach, stratigraphic cycles are essentially linked with styles of tectonism analogous to Phanerozoic tectonic environments (Eriksson et al., 1994). Eriksson et al., (1994) describes six general lithological associations in Archaean greenstone belts based on their dominant lithofacies components, which are possible analogues to some of the lithologies present at RGM: (1) Mafic-volcanic association; (2)

Calc-alkaline volcanic association; (3) Bimodal volcanic association; (4) Quartz-arenite-iron-formation and / or carbonate association; (5) Conglomerate-wacke association; (6) Conglomerate-arenite association. The distribution of rocks at RGM that can be grouped under different lithological associations is used later in this paper to elucidate the likely sequence of events responsible for the geology of RGM and has relevance to understanding the tectonic evolution of this enigmatic piece of the Guiana shield.

II B. Regional Geologic Background:

Suriname is located in the Guiana shield, a Paleoproterozoic massif of rocks in the northwest corner of South America between the Orinoco and Amazon river basins, to the north and south respectively (Figure 2.1; Gibbs and Barron, 1993). The majority of the Guiana shield is composed of granitic rocks associated with the Paleoproterozoic Transamazonian orogeny. Greenstone-belts are present, predominantly in the northern part of the shield between Venezuela and French Guiana, trend roughly NE-SW, and span a distance from north to south of about 200 kilometers (Figure 2.1). In Suriname and French Guiana, the greenstone belts, comprising the Marowijne and Maroni supergroups, respectively, are subdivided into two groups of rock. These are the Paramaka and the Armina Groups (Paramaca and Bonidoro in French Guiana). The Paramaka Group is mainly composed of metaigneous rocks, whereas the Armina Group is mainly composed of metasedimentary rocks. The Paramaka and Armina Groups are unconformably overlain by rocks of the Rosebel Group (Gibbs and Barron, 1993). The following table (after Gibbs and Barron, 1993) lists the Lower and Mid-Proterozoic rock formations in Suriname and their probable correlative groups in French Guiana, in their probable stratigraphic order.

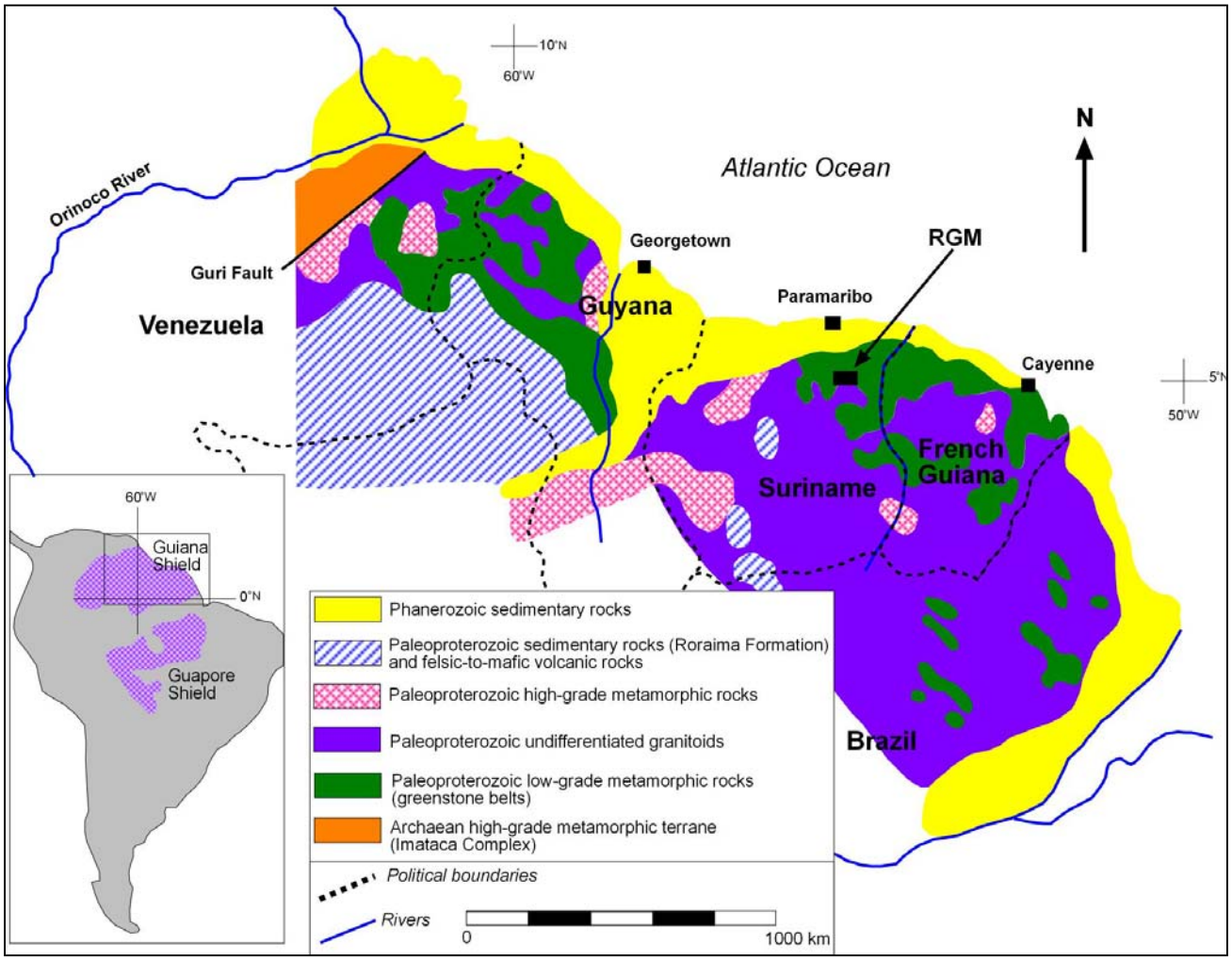

Figure 2.1: Location map and general geology of the Guiana Shield from Venezuela to Brazil. Modified from Voicu et al., (2001).

	Suriname	French Guiana
Mid-Proterozoic		
	Ston Formation (fluvial)	(Not found)
Lower Proterozoic		
?Molasse	Rosebel Group	Orapu Group
?Flysch	Armina Group	Bonidoro Group
Volcanic rocks	Paramaka Group	Paramaca Group

Table 2.1: General stratigraphic correlations between Suriname and French Guiana

The oldest rocks, of the Paramaka Group include amphibolitic metabasalt on the peripheries of granitoid rocks and gneiss of northeastern Suriname, and lower-grade metabasalt and intermediate to felsic volcanic rocks of the internal portions of the greenstone belt (Gibbs and Barron, 1993). The internal stratigraphy of the Paramaka Group has not been well established in Suriname, but Bosma et al. (1983) describe the overall stratigraphy of the Paramaca Group in French Guiana: The lower part of the Paramaca Group in French Guiana is a 1.5 kilometer thick sequence of tholeiitic metabasalt and metagabbro, which is overlain by 1-2 kilometers of gneiss derived from dacitic and rhyolitic tuff (Gibbs and Barron, 1993). The uppermost units of the Paramaka Group consists of mica-schist and aluminous gneiss, with dark, interbedded quartzite, iron-formation, and manganese-rich metasandstone, and these have a stratigraphic thickness of over 1 km (Gibbs and Barron, 1993).

Above the Paramaka Group is the predominantly sedimentary Armina Group (Bonidoro Group in French Guiana). The Armina Group forms a rhythmic sequence of graded greywacke and phyllite along the northeastern margin of the Paramaka Belt (Gibbs and Barron, 1993). Cross-bedding, ripple marks, and rhythmic, graded beds interpreted to be turbidites, are common features in the Armina Group (Gibbs and Barron, 1993). Bosma et al., (1983) found that the metasedimentary rocks of the Armina

Group consist mainly of quartz, altered plagioclase, and fragments of intermediate volcanic rock (Gibbs and Barron, 1993). Beds of wacke in the Armina Group have sharp basal contacts, sometimes with bottom-loading structures (Bosma et al., 1983 in Gibbs and Barron, 1993).

The Armina Group in Suriname is generally correlative with the Bonidoro Group in French Guiana (Gibbs and Barron, 1993). The contact between the Bonidoro Group and the underlying Paramaca Group is an unconformity (Gibbs and Barron, 1993). The Bonidoro Group includes quartzite, rhyolitic flows and tuff, aplitic microgranite, polymict basal conglomerate, schist, phyllite, greenish sandstone, and arkosic quartzite. The stratigraphic thickness of the formation is approximately 2-3 kilometers (Barroul, 1967; Brouwer, 1962 in Gibbs and Barron, 1993).

Above the Armina and Bonidoro Groups are the Rosebel and Orapu Groups. The Rosebel Group in Suriname includes immature sedimentary rocks, resting unconformably on the Paramaka Group, from which the sediments appear have been derived (Gibbs and Barron, 1993). Lithologically, the Rosebel Group consists of immature sandstone, conglomerate and phyllite, and in some cases, intercalated intermediate volcanics (Gibbs and Barron, 1993). The rocks of the Rosebel Group have undergone low-grade metamorphism, and are classified by Bosma et al., (1983) as medium-to-coarse-grained arenite, grading into arenitic graywacke, showing well-preserved sedimentary structures, predominantly ripple crossbedding (Gibbs and Barron, 1993). Pebbles in the conglomeratic intercalations are derived from the underlying Paramaka Group and typically preserve a foliation discordant with the matrix (Bosma et al., 1983). The rocks

of the Rosebel Group have not been seen overlying the Armina Group in Suriname, which is also thought to be derived from the Paramaka (Gibbs and Barron, 1993).

In French Guiana, The Orapu Group is composed of predominantly sedimentary with few volcaniclastic intercalations (Gibbs and Barron, 1993). An unconformity is reported at the base of the Orapu Group, evident through a siliceous regolith reflecting a period of continental weathering and erosion postulated at the top of the Bonidoro Group, along the Mana River (French Guiana), where the two groups are distinguished (Gibbs and Barron, 1993). The Orapu Group is well exposed in the eastern part of the northern greenstone belt of French Guiana, and includes metapelitic, locally carbonaceous schist, arkosic and quartz-rich sandstone, and polymict and quartz-rich conglomerate (Gibbs and Barron, 1993). The Orapu Group has a stratigraphic thickness of approximately 2 kilometers (Gibbs and Barron, 1993). Metamorphosed, polymict conglomerate and sandstone are commonly found in the lower part of the group whereas the upper part consists of metapelitic schist and intercalated sandstone (Gibbs and Barron, 1993). Clasts in the conglomerate are mainly of siliceous and pelitic clastic and chemical sedimentary rocks, and massive vein quartz (Gibbs and Barron, 1993).

II C. Local Formation Names:

There are still conflicting opinions among RGM geologists as to which of the previously mentioned groups are present at the RGM property and what these groups may or may not include. The following table lists historical and modern group and formation names, in order from oldest (bottom) to youngest (top), their geographic locations, and the rock types they include.

RGM formation name	Group name (Gibbs and Barron, 1993)	Formation name (Brinck, 1955)	Series (Brinck, 1955)	Location (RGM, and regional if available)	General description
Rosebel Formation	Rosebel Group (Suriname), Orapu Group (French Guiana)	Orapu Formation	Rosebel Series (A' Grossgroup)	Bedrock of the savannah area	Beige to white sandstone and conglomeratic sandstone. A' Grossgroup applied to the bedrock of the savannah area, which was thought to be the same lithology as the rest of the Rosebel series, but metasomatically altered (Brinck, 1955). Metapelitic, locally carbonaceous schists, arkosic and quartz-rich sandstones, and polymict and quartz-rich sandstones, thought to be molasse by Gibbs and Barron, (1993).
Armina Formation?	This would fall under the Rosebel Group according to Gibbs and Barron's description.	Orapu Formation	Rosebel Series	Proximal to volcanic rocks in the northern and southern flanks of the RGM concession	Conglomerates, wackes, and sericite-schists. The Rosebel series comprises most of the sedimentary rocks of the known gold deposits of RGM, excluding the bedrock of the savannah. These rocks are now known as the Armina Formation.
Armina Formation	Armina Group	Orapu Formation	Maabo Series	Donderbari hills	Phyllitic rocks with intercalated conglomerates
Armina Formation	Armina Group (Suriname), Bonidoro Group (French Guiana).	Balling Formation	Bonnidoro series	Donderbari hills. The Bonnidoro and Paramaka groups are distinguished on the Mana River in French Guiana (Gibbs	The Bonnidoro group includes quartzites, rhyolitic flows and tuffs, aplitic microgranites, polymict basal conglomerates, schists and phyllites, greenish sandstones and arkosic

				and Barron, 1993).	quartzites (Barroul, 1961 in Gibbs and Barron, 1993). Cross-bedding and ripple marks are common, and it has been described as unconformable on the Paramaka Formation.
Paramaka Formation	Paramaka Group	Balling Formation	Paramaka Series	North of the Donderbari Hill region, present south of the RGM concession and elsewhere in the Guiana Shield	Mainly Mafic igneous rocks with intercalated phyllitic sedimentary rocks in the upper part (Gibbs and Barron, 1993).
Paramaka Formation	?	Balling Formation	Nassau Series		

Table 2.2: Historic and modern rock formations names both regionally and in the RGM area

These formation names occur frequently in the literature but it is difficult to be sure what they are referring to in the context of the RGM rocks. For example, the Armina Group is now understood by some authors to include volcanic and volcaniclastic rocks, whereas these were originally classified as the Paramaka series of the Balling Formation. The greatest confusion has occurred over the Rosebel Group, which was originally given to most of the sedimentary rocks of the RGM area including the bedrock underlying the savannah sands. The "A' Grossgroup" was used by Brinck (1955) to distinguish the savannah-bedrock from the rest of the sedimentary rocks, which he though were of the same origin, but experienced different types of metasomatic alteration. Armina Formation has become a poorly defined term at RGM, in that the opinions of RGM geologists vary as to what the formation includes, and is presently used to describe volcanic, volcaniclastic, and sedimentary rocks (excluding those of the savannah), which historically would have fallen under the Paramaka and Orapu Formations respectively.

Regardless of the confusion among formation names in the literature, there are at least four different types of sedimentary units present at RGM that have unique characteristics and represent different types of depositional environments during the Paleoproterozoic, preserved in the stratigraphic record of RGM. These rocks are composed of different types of clasts, and have different textures. Analyses of clast compositions and sedimentary structures of the sedimentary rocks of RGM, combined with geochemical analyses of volcanic rocks of RGM are critical in developing an interpretation of the sequence of events that took place prior to, and during the Transamazonian orogeny.

III. Rosebel gold mine rock types:

Introduction:

Rock exposures at RGM are generally restricted to mine-pits, exploration targets, areas where diamond drilling has been carried out, and less commonly, outcrops (Plate 1). Data from five locations on the RGM property are discussed in the following sections of this paper, and are listed in order of relative probable age, based on field relationships, petrographic analyses, and trace element geochemistry of igneous rocks. Igneous rocks comprise the base of the stratigraphic sections in four out of five deposits, and are discussed first, followed by arc-related sedimentary rocks, recycled orogenic sedimentary rocks, and finally, younger intrusive rocks.

III. A. Paleoproterozoic igneous rocks:

Analytical methods:

Initially, I used field mapping and studies of diamond drill-core, in addition to previously compiled drill-core data, in order to assess the relevance of different igneous rock types at RGM to this study. These field studies, carried out by me and other geologists at RGM, were used in selecting rocks for whole-rock and trace element ICP mass-spectrometry, carried out by ALS Chemex laboratories in Sudbury Ontario. Samples of hard rock were prepared and analyzed by ALS following this procedure: (1) Initial weighing, drying, and fine crushing of entire sample to at least 70% 2 millimeter grain-size; (2) Split off 250 grams and pulverize split to at least 85% <75 micron grain

size; (3) Lithium borate fusion of the sample; (4) Digestion in acids; (5) Whole rock and trace element analysis through ICP-MS.

Most of the rocks in this study have been metamorphosed to low to mid greenschist grade. Therefore, high-field-strength trace elements (HFSE), characterized by cations with small ionic radii to ionic charge, are used to categorize the igneous rocks of RGM in terms of their original magmatic source, as these elements are generally immobile during metamorphism (e.g. Woodhead et al., 1993).

III. A. 1. Basalt of the Royal Hill deposit:

The Royal Hill gold deposit lies along the southern part of the RGM concession and spans an area of roughly 4 square kilometers. The rocks of the Royal Hill gold deposit consist of mafic volcanic rock, lapilli tuff and volcanic breccia, and fine-grained tuff, comprising a unit of approximately 400 meters in width, which is unconformably overlain by wacke with intercalated polymict conglomerate, spanning a geographic distance of approximately 575 meters (Plate 1).

Mafic igneous rocks make up the stratigraphic base of the Royal Hill deposit. These rocks are aphanitic to phaneritic, sometimes tuffaceous, and form a dark-purple saprolite in the upper weathering profile. Fresh rock is generally dark green to gray, fine-to-medium-grained material. In some cases, visible crystals of plagioclase, augite, and magnetite, are present. Chloritized amphibole porphyroblasts, and sericite-carbonate porphyroblasts are also present in some samples. The rock is generally strongly foliated. Healed crackle-breccia is present in some drill-core samples, especially in proximity to the contact between the volcanic and sedimentary rock. Metasomatic alteration is

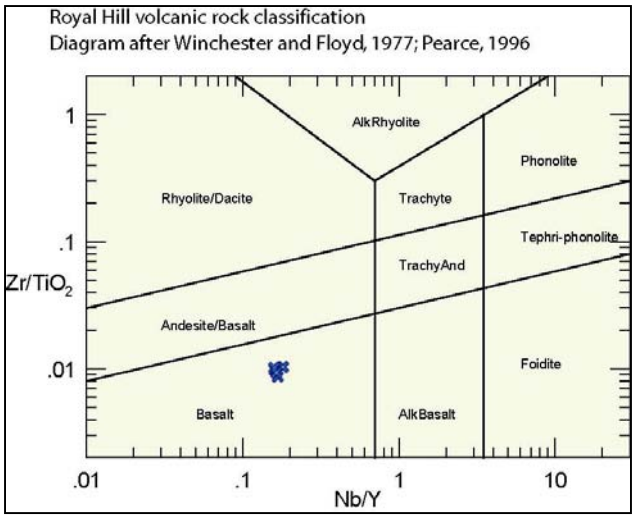

Figure 3.1: Tectonomagmatic discrimination diagram of Royal Hill volcanic rocks, based on HFSE, indicating basaltic provenance.

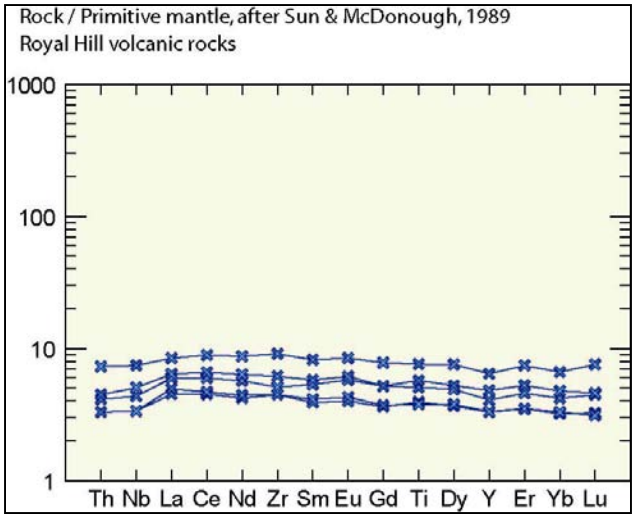

Figure 3.2: Spider diagram of trace element content for Royal Hill volcanic rocks, normalized to primitive mantle composition.

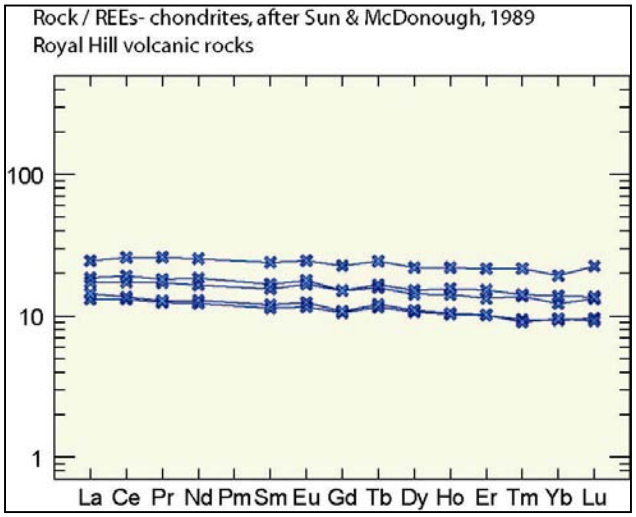

Figure 3.3: Rare Earth element diagram (normalized to chondrites) of the Royal Hill volcanic rocks. Note the 20 to 30-fold level of enrichment in all REE's, and the lowest level of enrichment in the incompatible elements in comparison to the other igneous rocks in this study.

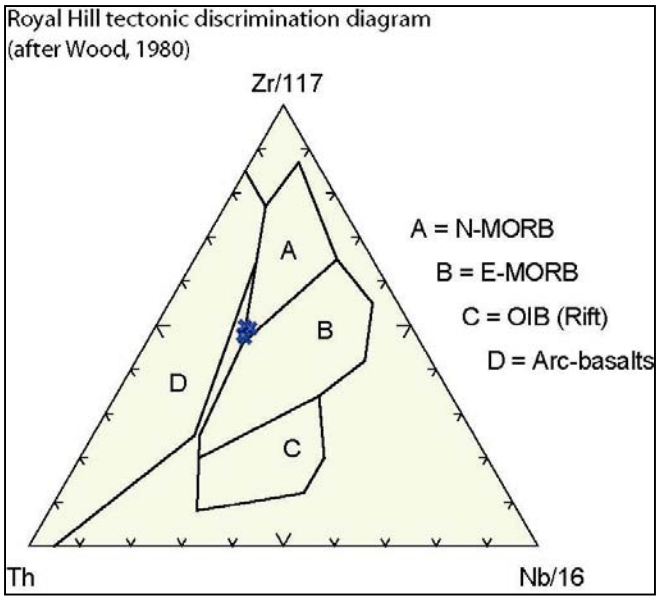

Figure 3.4: Tectonomagmatic discrimination diagram based on HFSE of Royal Hill rocks.

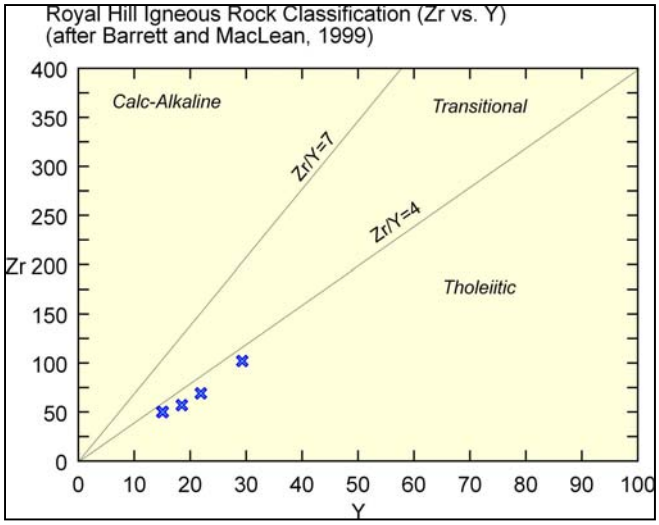

Figure 3.5: Harker diagram of Y vs Zr, indicating tholeiitic affinity of Royal Hill volcanic rocks.

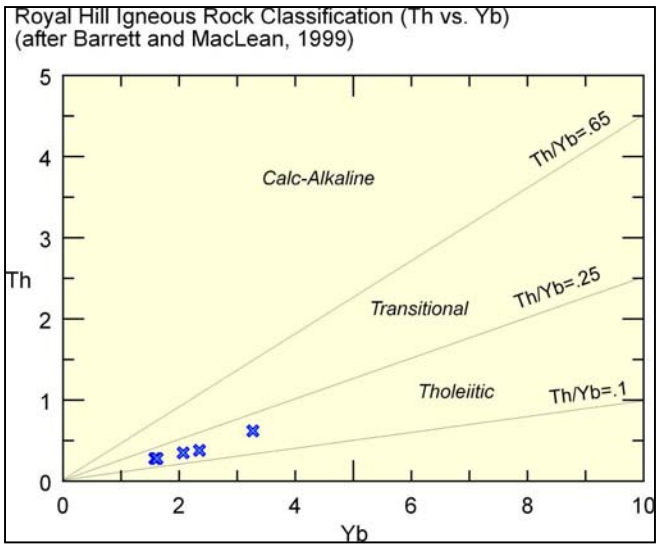

Figure 3.6: Harker diagram of Yb vs Th, indicating tholeiitic affinity of Royal Hill volcanic rocks.

common in these rocks, especially in proximity to quartz veins. Alteration features typically include silicification, sulphide minerals, carbonate, and tourmaline.

Ratios of Zr/TiO_2 versus Nb/Y obtained from these rocks are consistent with basalts (Figure 3.1; Winchester and Floyd, 1977; Pearce, 1996). Plots of rare earth elements (REE's), for these rocks show the lowest level of enrichment in incompatible elements of all the igneous rocks in this study, yet still show a 10 to 20 fold level of enrichment in REE's, when compared to chondrites (Figures 3.2 and 3.3). The volcanic rocks of the Royal Hill deposit are the most mafic rocks identified at RGM. Ratios of Zr/Y, and Th/Yb are in the tholeiitic range (Figures 3.5 and 3.6; Barrett and MacLean, 1999).

Because the volcanic rocks of Royal Hill are the most mafic rocks identified in this study, they should probably be classified with the Paramaka Group, which is reported in French Guiana to include tholeiites (Vanderhague et al., 1998). Ratios of Th, Nb/16, and Zr/117, when plotted on a ternary diagram devised to characterize tectonomagmatic provenances of mafic rocks (Figure 3.4; Wood, 1980) do not show a conclusive provenance for these rocks. However, the enrichment in rare earth elements of the Royal Hill basalt, and the flat slope of the plots of REE's, normalized to chondrites (Figure 3.3) is consistent with some other Paleoproterozoic arc-related basalts elsewhere in the world (e.g. Wang et al., 2004). Rocks of this type were not previously identified in the southern area of the RGM property.

Tholeiitic rocks are noted in Archaean and Proterozoic greenstone belts, and usually occur towards the base of the sequences. The Rio das Velhas greenstone belt, in Brazil (Baltazar and Zucchetti, 2005), and the Birimian greenstone-belts in west Africa

(Attoh and Ekweume, 1997) are two (of many) examples, where this is the case. The Birimian greenstone belts in West Africa are the most important example, because they are also thought to be related to the Transamazonian orogeny (Eburnean orogeny in Africa) (Ledru et al., 1994).

III. A. 2. Andesite to basalt of the Pay Caro and north-trend deposits:

The Pay Caro and East Pay Caro gold deposits are located along the southern flank of mafic to intermediate igneous rocks found to the south of the so-called north-trend gold deposits (Plates 1 and 4). The deposits lie along a roughly 110° trend of approximately 3 kilometers in length, and are associated with the contact between the volcanic rocks to the north, and sedimentary rocks to the south. To the north of the igneous rocks, north of Pay Caro, are three deposits that comprise the so-called north-trend of mineralization. These deposits, "Koolhoven," "J-zone," and "Spin-zone," from west to east respectively, span a distance of about ten kilometers from northwest to southeast, and two kilometers from north to south (Plates 1 and 4). These deposits are bordered to the north by mafic igneous rocks.

The igneous rocks to the south of the three north-trend deposits, and to the north of the Pay Caro deposit (Plates 1 and 4), span a distance from north to south of approximately 1.1 kilometers, and include a variety of igneous textures, from aphanitic to phaneritic, and in some cases porphyritic and tuffaceous. The rocks are generally dark gray-blue to gray-green in hand sample. Pillow structures have been observed in the saprolite of these rocks, indicating that they are related to subaqueous volcanism.

As expected with greenschist-grade metamorphism, epidote, chlorite, and carbonate are common secondary minerals in these rocks. Chlorite-carbonate

porphyroblasts are sometimes present, especially in the aphanitic and tuffaceous rocks. Geochemical analyses indicate that the Zr/TiO_2 versus Nb/Y ratios are in the andesite to basalt compositional range (Figure 3.7; Winchester and Floyd, 1977; Pearce, 1996). Plots of trace elements, normalized to primitive mantle composition, and REE's normalized to chondrites (Figures 3.8 and 3.9; Sun and McDonough, 1989), show enrichment in incompatible trace elements in these rocks, indicating a subduction component to the magma. Interpretation of HFSE (Th, Nb, Zr) distributions indicate that these rocks are probably arc-related (Figure 3.10; Wood, 1980). Ratios of Zr/Y, and La/Nb are in the range of rocks with transitional to calc-alkaline affinities (Figures 3.11 and 3.12; Barrett and MacLean, 1999).

The intermediate igneous rocks of Pay Caro show a more calk-alkaline affinity than the rocks of Royal Hill. These rocks probably represent a more advanced phase of arc-related volcanism than the Royal Hill rocks, as the greater enrichment in incompatible elements indicates a greater slab component to the magma.

Igneous rocks are also present to the north of the north-trend. However, fresh rock does not crop out in this location, nor has it been drilled through, due to the fact that it is mainly beyond the exploration limits of the RGM property. These rocks have historically been considered a member of the Balling Formation (Paramaka equivalent) (Brinck, 1955), which mainly consists of basalt and mafic tuff. The volcanic rock is identified in the field as a deep red and purple, massive, aphanitic to coarse-grained, and in some areas, tuffaceous saprolite, similar in appearance to that encountered at Royal Hill.

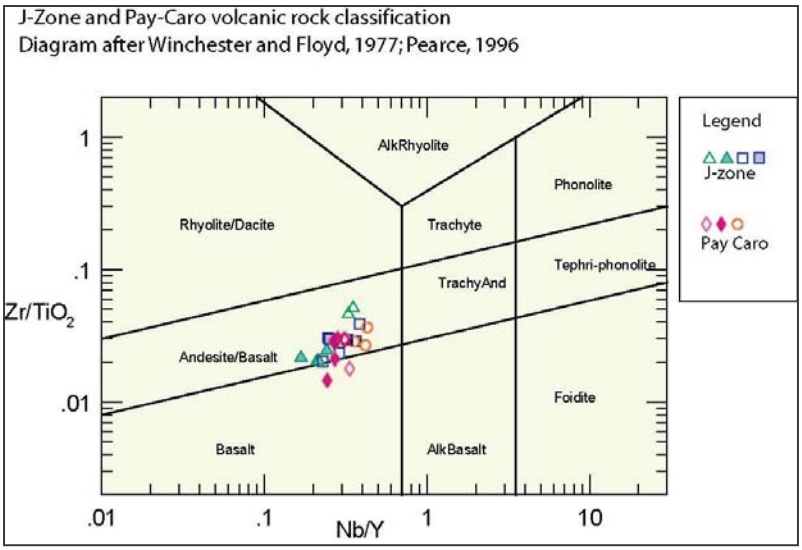

Figure 3.7: Tectonomagmatic discrimination diagram of J-zone and Pay Caro volcanic rocks, based on HFSE, indicating andesitic to basaltic provenance.

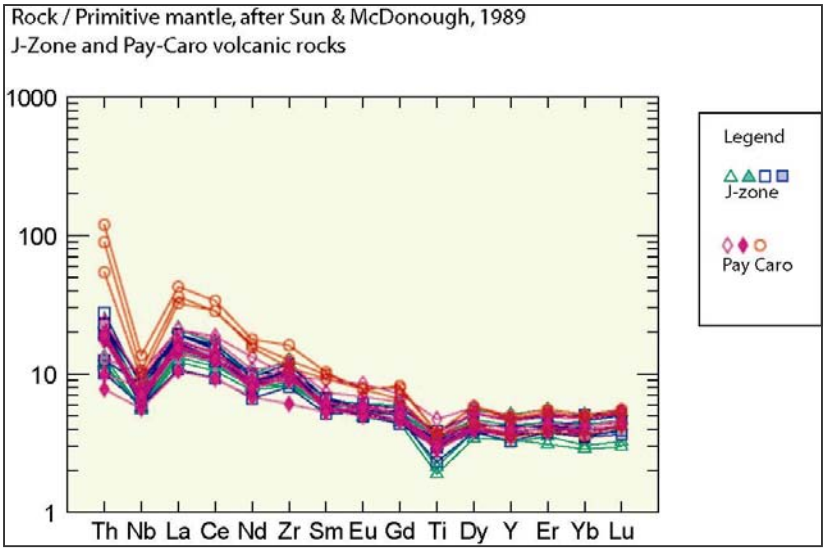

Figure 3.8: Spider diagram of trace element content for J-zone and Pay Caro volcanic rocks, normalized to primitive mantle composition.

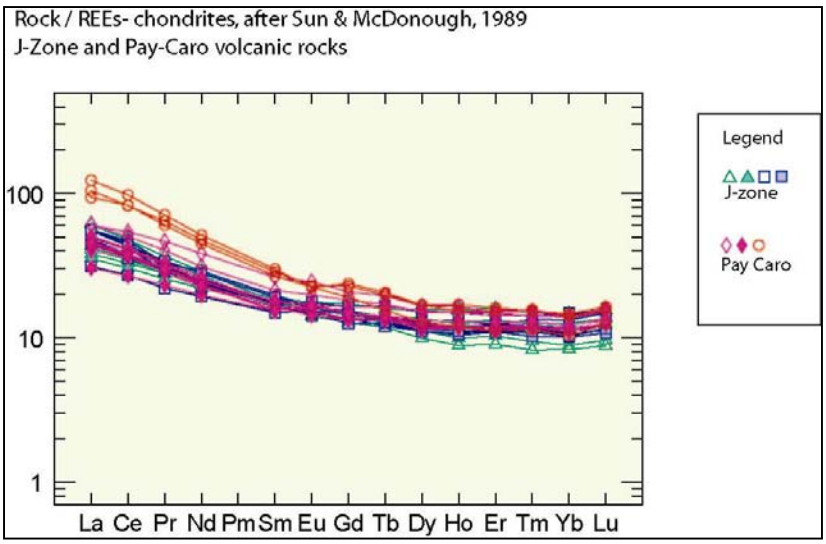

Figure 3.9: Rare Earth element diagram (normalized to chondrites) of the J-zone and Pay Caro volcanic rocks. Note the intermediate level of enrichment in incompatible elements, in comparison to the other igneous rocks in this study.

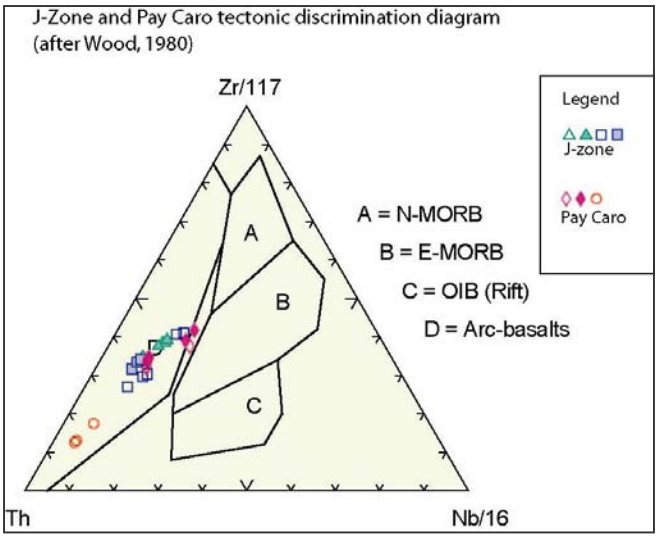

Figure 3.10: Tectonomagmatic discrimination diagram based on HFSE of J-zone and Pay Caro volcanic rocks indicating a volcanic arc association.

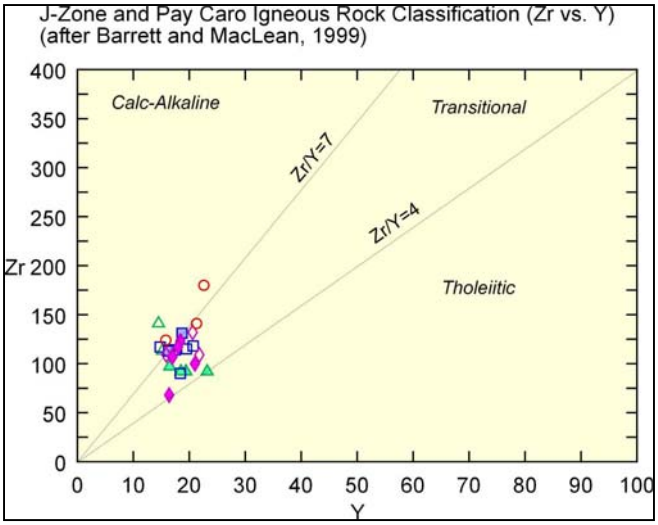

Figure 3.11: Harker diagram of Y vs Zr, indicating transitional to calk-alkaline affinity of J-zone and Pay Caro volcanic rocks.

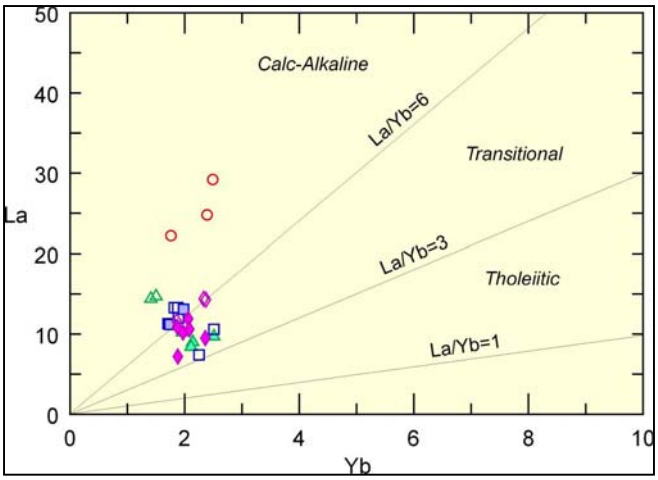

Figure 3.12: Harker diagram of La vs Yb, indicating transitional to calk-alkaline affinity of J-Zone and Pay Caro volcanic rocks.

The igneous rocks to the north of the north-trend appear to be conformably overlain by a fine-grained turbiditic sedimentary rock. This may indicate deposition of volcanic source material in a pelagic environment, possibly a submarine ramp in a forearc or back arc basin setting. If this is the case, then the volcanic rocks to the north of the turbiditic sediments should either be back arc basin basalts or mid ocean ridge basalts. Trace element geochemistry could be used to elucidate this concept, if samples of these rocks should become available through RGM.

III. A. 3. Felsic to mafic volcanic rocks of the Mayo - Roma deposits:

The Mayo deposit is located 4 kilometers WSW of the Royal Hill deposit, and is believed by mining geologists to be located along the same "south-trend" of mineralization. The stratigraphy of the Mayo deposit begins with an unconformable contact between-mafic-to felsic volcanic rocks at the south end of the deposit, and a conglomeratic wacke. Felsic volcanic rocks comprise the stratigraphic base of most of the western part of the deposit, with a subordinate presence of mafic volcanic rocks to the east.

The felsic volcanic rocks have Zr/TiO_2 versus Nb/Y ratios consistent with rhyolite and dacite (Figure 3.13; Winchester and Floyd, 1977; Pearce, 1996), and are typically massive, dull gray aphanites in hand-sample. In some cases, flow breccias are present, especially near the contact with the overlying sediments. In the eastern part of the Mayo deposit are more mafic volcanic rocks, that have Zr/TiO_2 versus Nb/Y ratios consistent with basalt and andesite (Figure 3.13; Winchester and Floyd, 1977; Pearce, 1996). Trace element geochemical analyses of these rocks indicate that they are probably arc-related as illustrated by Figures 3.14, 3.15, and 3.16, as they are very enriched in incompatible

REE's. Ratios of Y/Zr, and Yb/Th from the mafic and felsic volcanic rocks of Mayo are in the transitional to calc-alkaline ranges respectively (Figures 3.17 and 3.18; Barrett and MacLean, 1999).

Compositions of the igneous rocks from Mayo show the highest level of enrichment in incompatible REE's, in comparison to the other rocks in this study, and show a similar level of enrichment to a granite, located to the southeast of the Mayo deposit. The Mayo deposit rocks seem to show the most calk-alkaline affinity as well. It is a contention of mining geologists at RGM that the Mayo and Royal Hill deposits are situated along the same so-called south-trend of mineralization. However, the differences in the volcanic rocks of the two deposits do not support this notion. Unfortunately, there is not a great deal of information (known to the author at least), aside from the aerial magnetic survey data, in the swath of land between the two deposits (spanning a distance of about 2.5 kilometers). So it cannot be said with any assurance why these two clearly different deposits are in proximity to one another.

Lowe (1994) discusses some aspects of Archaean felsic-intermediate volcanic-terrigenous rocks that bear relevance in understanding the Mayo deposit. The felsic volcanic terrigenous association (FVT) includes high-standing, subaerial stratovolcanoes and volcanic complexes, with associated uplifts of underlying portions of greenstone-belt sequences, and locally exposed subvolcanic plutons providing major sources of compositionally varied debris to the local and regional sedimentary systems (Lowe, 1994). The FVT association includes rocks deposited sufficiently close to the volcanic centers, consisting of predominantly volcanic or juvenile pyroclastic and autoclastic rocks (Lowe, 1994). Felsic volcanic units include those erupted under relatively

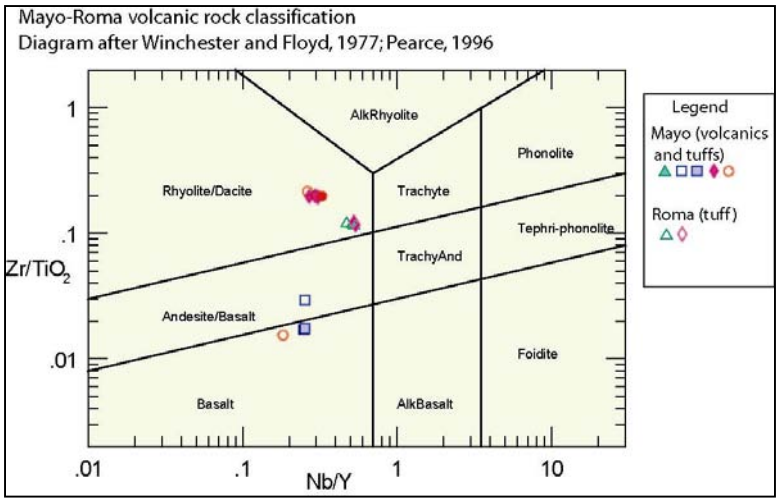

Figure 3.13: Tectonomagmatic discrimination diagram of Mayo-Roma volcanic rocks, based on HFSE, indicating bimodal (mafic and felsic) provenance.

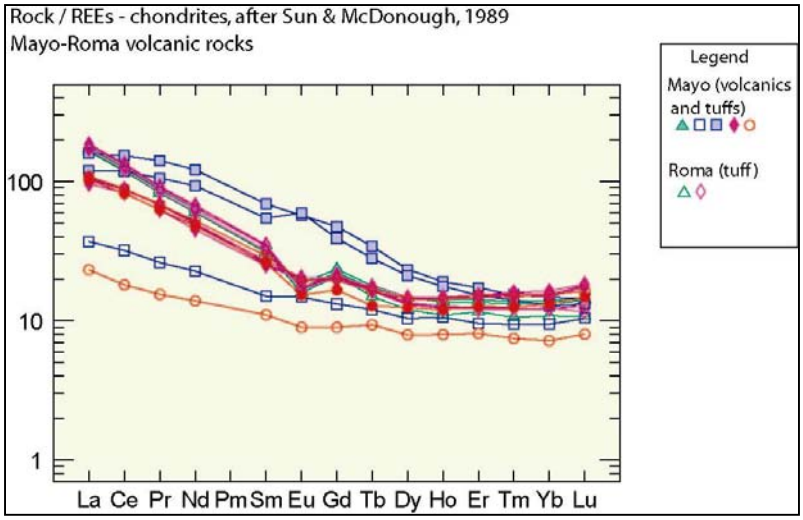

Figure 3.14: Spider diagram of trace element content for Mayo-Roma volcanic rocks, normalized to primitive mantle composition.

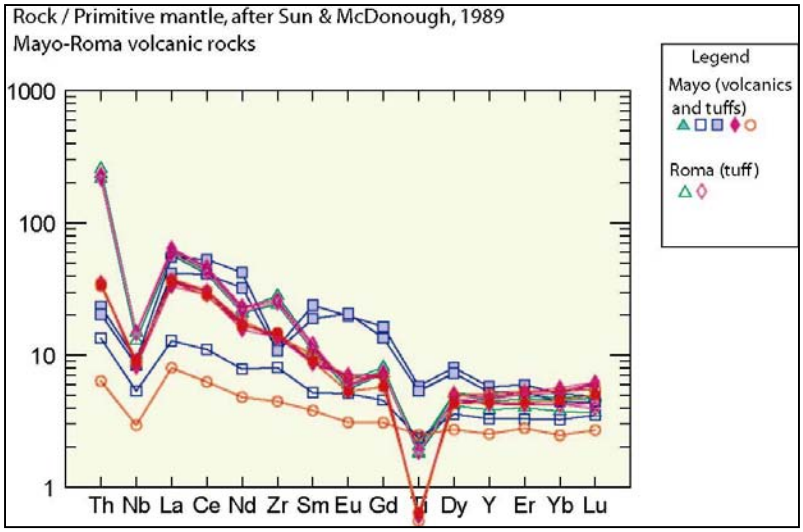

Figure 3.15: Rare Earth element diagram (normalized to chondrites) of the Mayo deposit felsic igneous rocks. Note the relatively high enrichment in incompatible elements, in comparison to the other igneous rocks in this study.

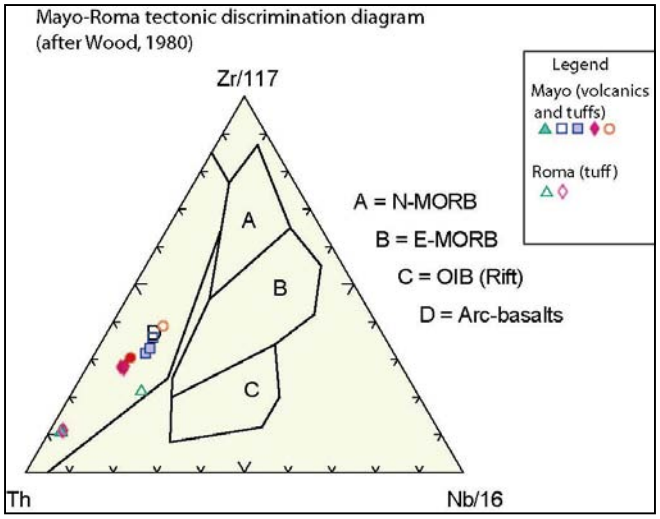

Figure 3.16: Tectonomagmatic discrimination diagram based on HFSE of Mayo-Roma volcanic rocks indicating a volcanic arc association.

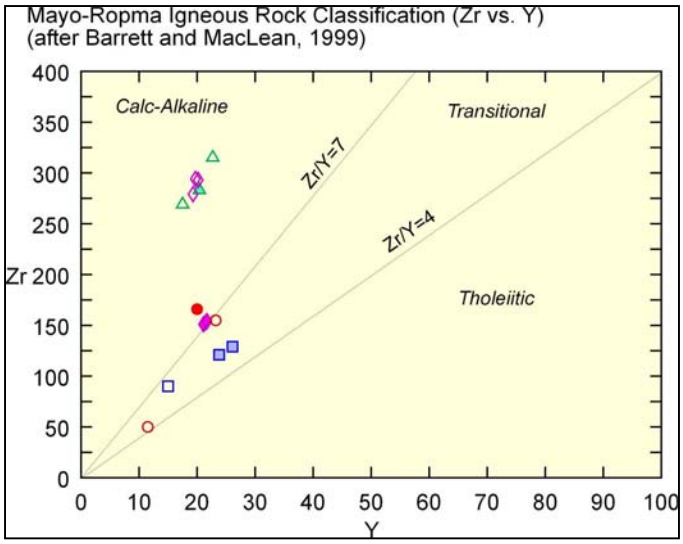

Figure 3.17: Harker diagram of Y vs Zr, indicating transitional to calk-alkaline affinity of Mayo-Roma volcanic rocks.

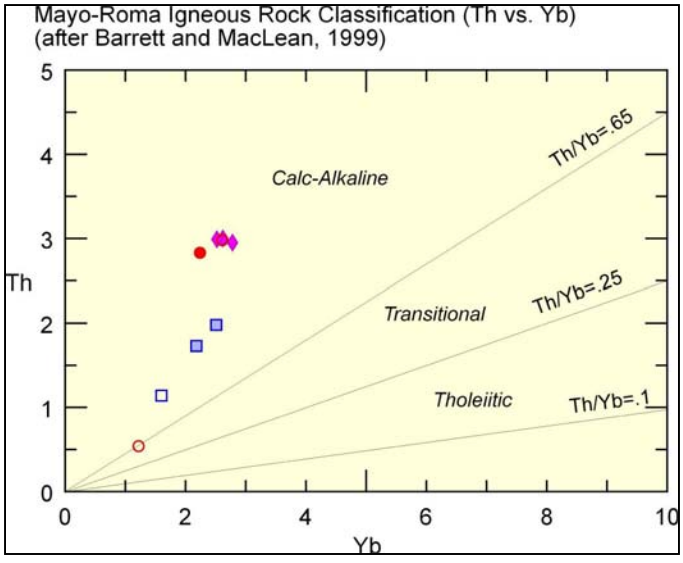

Figure 3.18: Harker diagram of Yb vs Th, indicating transitional to calk-alkaline affinity of Mayo-Roma volcanic rocks.

anorogenic conditions and composed of oligomict felsic volcanic and volcaniclastic materials as well as others containing debris derived from uplift of underlying portions of greenstone belts, subvolcanic plutons, and even older, pre-greenstone belt rocks (Lowe, 1994). This description seems to be a likely explanation for the sedimentation at Mayo, in which felsic material and (probably older) mafic material form debris flow conglomerates.

III. B. Paleoproterozoic sedimentary rocks:

Mafic to felsic igneous rocks comprise the stratigraphic base of all of the deposits of the RGM concession, with the exception of the Rosebel deposit. The sedimentary rocks overlying the lower volcanic units generally consist of fining upward sequences, from basal conglomerates to conglomeratic wackes, to siltstones and mudstones. The sedimentary rocks range in provenance from undissected arc, to recycled orogenic. Most of the sedimentary rocks at RGM have characteristics of syn-orogenic deposits in which primary erosive byproducts of volcanic rocks are rapidly deposited. These sedimentary deposits are discussed below.

Analytical methods:

Field-mapping and hand-sample observation of outcrops and diamond drill-core was first used in classifying the sedimentary rocks in this study. Core logging, and clast counting in the coarser grained rocks was then carried out in identifying different conglomerates, and in the selection of samples for thin sections. Point-counts of 200 grains from a total of 88 thin sections were then used to further classify conglomerate clasts, and to identify the tectonic provenance of the finer grained rocks.

The technique of classifying sandstones in terms of tectonic provenance, devised by Dickinson (1983) is used to classify some of the wackes and pebble conglomerates discussed below. This method of classification categorizes sandstones based on their quartz, feldspar, and lithic fragment contents in order to assess the stage of orogenesis that the sediments are related to. Ternary diagrams (commonly referred to as QLF diagrams) of quartz, lithic fragments, and feldspar, based on point-counts of Phanerozoic sandstones in North America from known tectonic provenance (by Dickinson et al., 1983), are used to empirically classify sandstones of uncertain provenance in this study, by comparing them to sandstones of known tectonic provenance.

III. B. 1: Arc-related sedimentary rocks:

III. B. 1. A. North-trend sedimentary rocks:

The sedimentary rocks of the "north-trend," which are host to the "Koolhoven," "J-zone," and "Spin-zone" gold deposits, from west to east respectively, span a distance of about 10 kilometers in length and 2 kilometers in width that trends approximately 110° (Plates 1 and 4). Sedimentary rocks associated with the north-trend deposits consist of conglomerate, conglomeratic wacke, and conglomeratic siltstone-mudstone. These rocks have historically been classified as a member of the Armina Group, and previously as the Orapu Formation or Balling Formation (e.g. Ijzerman, 1931; Brinck, 1955).

The sedimentary rocks appear to conformably overlie mafic volcanic rocks to the north, with intercalated units of mafic tuff and mudstone. The sedimentary rocks of the north trend consist of strongly foliated turbiditic mudstones, and fine-to-coarse-grained wacke, composed of predominantly volcaniclastic lithic components in a matrix of sericite, chlorite, and carbonate. The wacke is texturally and mineralogically immature

(Folk, 1964), with angular to sub-angular clasts of lithic fragments. Layers of matrix-supported, pebble to cobble-sized conglomerate are present in the mudstones and wackes, and form beds ten to thirty centimeters thick in the mudstone units, and several meters thick in the wacke. Clasts in the conglomerate and conglomeratic wacke consist mostly of felsic porphyritic and felsic aphanitic volcanic fragments, with subordinate monocrystalline quartz, mafic volcanic fragments, and feldspathic fragments, with matrix material similar to that of the wacke mentioned above (Figure 3.19).

All of the sedimentary rocks of the north trend show evidence of graded bedding, consistent with Bouma horizons C-D, and D-E (Boggs, 2001). Cross-bedding and graded beds generally indicate a top to the south polarity, however this may be misleading due to the fact that these rocks are highly folded. Syn sedimentary deformation features, such as slumps and de-watering structures have been observed in the wacke of the north trend. QLF and QmLtF diagrams obtained from point-counts of 200 grains from 25 thin sections from the north trend rocks are consistent with those of sedimentary rocks of undissected island-arc provenance (Figure 3.20).

The sedimentary rocks of the north-trend have a proximal-to-distal-turbidite lithofacies association, with mafic and felsic clastic source material, indicating that these rocks were deposited in a deep-water, tectonically active basin. Petrographic analyses of thin sections from turbiditic wackes of the north-trend rocks indicate an arc association, and analyses of clast compositions of conglomerates support a mafic to felsic sediment source (Figure 3.19).

Eriksson et al., (1993) discuss some examples of arc-related sedimentary associations in the Canadian Shield and their probable depositional environments that are

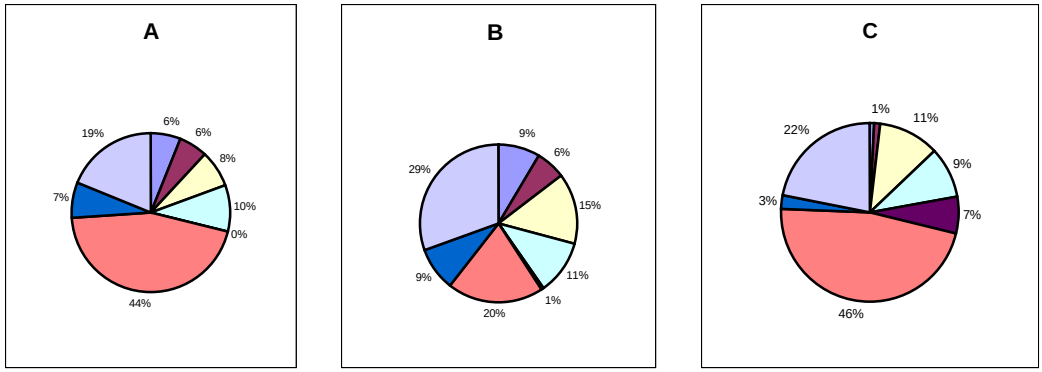

Figure 3.19: (A) Pie chart indicating clast population of conglomerate from the Koolhoven deposit; (B) Pie chart indicating clast population of conglomerate from J-Zone; (C) Pie chart indicating clast population of conglomerate from Spin-Zone, Based on petrographic and field analyses.

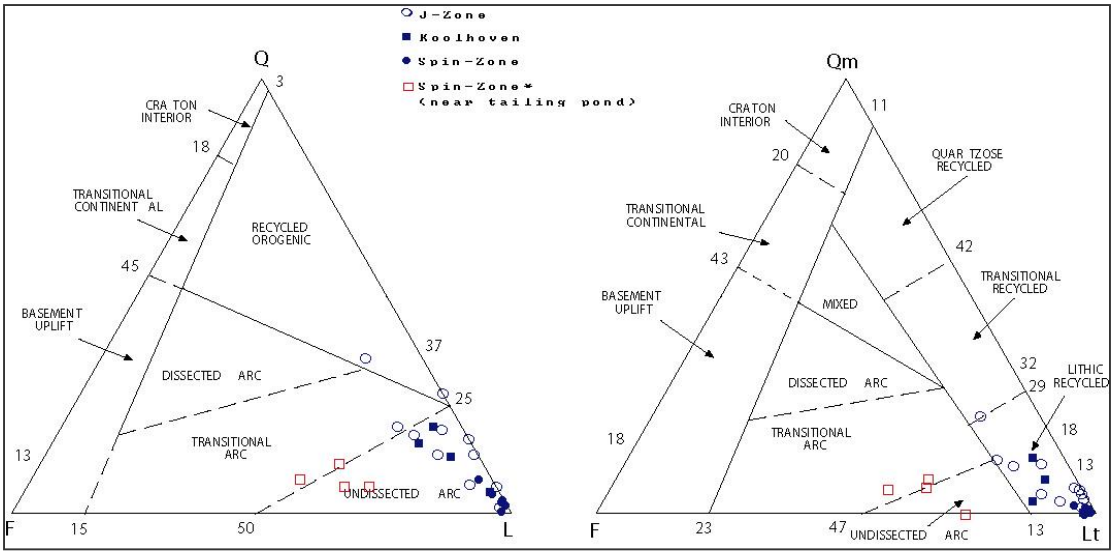

Figure 3.20: (left) Ternary diagram of quartz (Q), feldspar(F), and lithic-fragment(L) content of wacke from Koolhoven, J-Zone, and Spin Zone; consistent with undissected-arc provenance (Based on Dickinson, 1983). (right) Ternary diagram of monocrystalline quartz (Qm), feldspar(F), and lithic-fragment(Lt) content of wacke from Koolhoven, J-Zone, and Spin-Zone; also consistent with transitional arc provenance (Based on Dickinson, 1983). Diagrams based on point-counts of 200 grains from 21 thin sections of conglomeratic wacke and matrix supported conglomerate from the North-trend rocks (Koolhoven, J-Zone, and Spin-Zone).

Figure 3.21: Photograph of matrix-supported conglomerate of the north trend. Cutlass for scale (~4.5 cm across at hilt).

Figure 3.22: Photograph of turbiditic wacke of the north trend. Pencil indicates stratigraphic up.

possible analogues to the sedimentary rocks at RGM. The types chosen are: a fore-arc-slope trench assemblage, a rifted island arc, and a mature island-arc. Their respective settings are: the Beardmore-Geraldton area in the Wabigoon and Quentico Subprovinces, the Schreiber-Hemlo area in the western Abitibi Subprovince and the Shebandowan region of the western Abitibi Subprovince (Eriksson et al., 1993). The metasedimentary rocks are present in 3 belts: the northern metasedimentary belt (NMB); central metasedimentary belt, (CMB); and southern metasedimentary belt (SMB) (Eriksson et al., 1993). These are 1-to-7 kilometer-wide belts, and are separated from each other by thick sequences of mostly mafic, pillowed and massive, tholeiitic volcanic rocks.

An extensive study of clast provenance in conglomerates of the NMB and the CMB, undertaken by Devaney (1987) reveals that felsic-to-mafic volcanic clasts dominate, forming over 75% of the clasts in most samples, with the remainder being composed almost entirely of porphyries or granitoids (Eriksson et al., 1994). These data indicate that the sediments were first-cycle, and derived from an extrusive-intrusive complex (Eriksson et al., 1994). The depositional environment of the conglomerates and sandstones of the NMB and northern CMB is described by Eriksson et al. (1994) as a fluvial fan or braidplain that drained an active volcanic region to the north. In this setting, gravely deltas in intervening areas fed sediments directly into a deeper marine source, where turbidites were deposited into a broad, laterally continuous ramp (Eriksson et al. 1994). Clast populations in this study seem similar to those encountered in the north-trend rocks, and the type of environment described is a probable explanation for the turbiditic sandstones with intercalated conglomerates present in the north-trend rocks of RGM.

The turbidite facies association in the north-trend rocks of RGM is also similar to a turbiditic association described in the upper volcano-sedimentary succession of the Paleoproterozoic rocks of the Boromo-Goren greenstone belt in Burkina Faso (in rocks comprising the Birimian Domain of the West African Craton), as described by Hein et al. (2004): The upper volcano-sedimentary succession consists of thick to thin beds of siltstone, shale, feldspathic quartzite – "gritstone," gravel to boulder sized meta-conglomerate, and immature volcanic breccia and tuff (Hein et al., 2004). The rocks are turbiditic, and part of a Bouma turbidite sequence is present, including laminations, cross laminations, dewatering structures, and rare scour and load structures (Hein et al., 2004). Fine-scale graded bedding, parallel and convoluted laminations, and rare slumps are sometimes present in the finer-grained units (Hein et al., 2004). Quartzite units are laminated, planar bedded, or cross-bedded in some locations, although the quartzites are generally massive. Volcanic breccia, meta-conglomerate, and meta-boulder conglomerate are generally matrix supported and contain angular, or oblong-shaped boulders up to 15 centimeters in diameter (Hein et al., 2004). The Birimian is probably the more relevant analogue, as it is also related to the Transamazonian orogeny, and therefore probably has a similar history to the rocks in the Guiana Shield.

III. B. 1. B: Royal Hill conglomerate and wacke:

The stratigraphy of the Royal Hill deposit begins with mafic to intermediate volcanic and volcaniclastic rocks that are unconformably overlain by a basal conglomerate with intercalated wacke. The Royal Hill conglomerate is poorly sorted, and consists of dominantly quartzite and mafic volcanic clasts, some felsic volcanic clasts, porphyritic felsic volcanic clasts, and some monocrystalline quartz and feldspar

(Figure 3.23). The coarser-grained conglomeratic units are poorly sorted and strongly foliated. Clast size in the conglomerates generally ranges from 2 to 7 centimeters, and averages around 5 centimeters. Quartz clasts are most representative of original clast morphology, and are sub-rounded to rounded, whereas less stable lithic clasts are often highly elongate due to shearing.

The conglomerates generally contain intercalated beds of wacke of between approximately 20 to 100 centimeters in thickness. Intercalations of wacke and coarse grained, moderately sorted pebble conglomerate are common. Pebble conglomerate and wacke of Royal Hill are composed of felsic volcanic clasts, feldspar, mafic volcanic clasts, and monocrystalline quartz, in a sericite, chlorite, carbonate, epidote matrix (Figure 3.23). Clasts in the pebble conglomerate are sub-rounded, and range in size from 2-8 millimeters.

The wacke of Royal Hill is poorly sorted, with grains ranging in size from 2-3 millimeters to clay-sized particles. Plagioclase in the wacke is commonly sausseritized, and dynamic recrystalization is evident in quartzite clasts. Matrix material typically consists of chlorite, carbonate, and quartz. Detrital magnetite and hematite comprise 2-3% of the Royal Hill wacke, and often form small-scale crossbeds. Polarity structures found in the crossbeds generally indicate that north is up.

Following Dickinson's (1983) technique, point counts of 200 grains from 6 thin sections of conglomeratic wacke from Royal Hill illustrate that the wacke is of undissected to transitional arc provenance, as the clasts are predominantly unstable lithic fragments (Figure 3.24). The basal conglomerates and immature wackes of the Royal Hill deposit are considered by mining geologists to be part of the Armina Group.

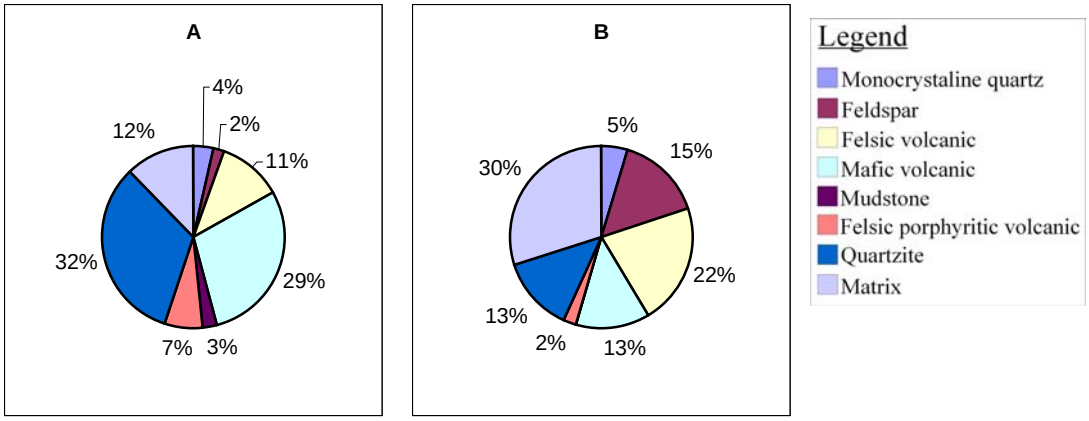

Figure 3.23: (A) Pie chart indicating clast population of basal conglomerate from the Royal Hill deposit, based on point counts of 200 grains from 9 thin sections and analyses of diamond-drill core (counts of clasts per interval of core). (B) Pie chart indicating clast population of conglomeratic wacke from the Royal Hill deposit, based on point-counts of 200 grains from 6 thin sections and analyses of diamond-drill core as mentioned above.

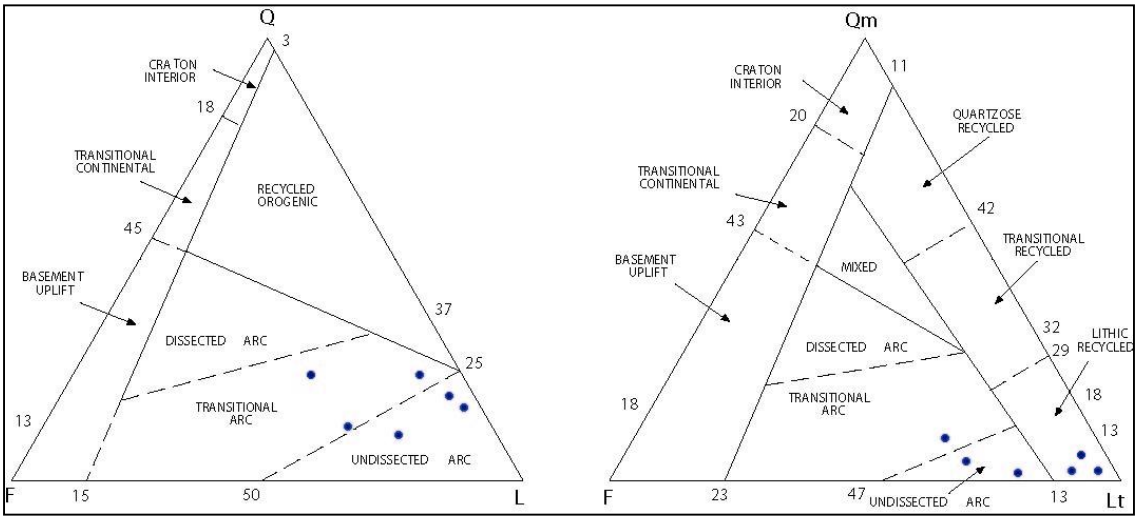

Figure 3.24: (left) Ternary diagram of quartz (Q), feldspar(F), and lithic-fragment(L) content of wacke from the Royal Hill deposit; consistent with undissected to transitional arc provenance (Dickinson, 1983). (right) Ternary diagram of monocrystalline quartz (Qm), feldspar(F), and lithic-fragment(Lt) content of wacke from the Royal Hill deposit; consistent with transitional to undissected arc, and lithic recycled provenances (Based on Dickinson, 1983). Diagrams based on point counts of 200 grains from 6 thin sections of wackes from the Royal Hill deposit.

The wacke of Royal Hill sharply contacts a more arenitic sedimentary unit to the north of the northwest Royal Hill pit, interpreted by RGM geologists as the Rosebel Group. Saprolite exposures of this rock are off-white to beige, and contain more quartzite than the wacke below. The contact between the two units appears to be a fault in the field, and corresponds to highly sheared intervals within diamond drill core. However, field data is lacking as to the orientation of this fault.

The sedimentary rocks of Royal Hill are consistent with a conglomerate-wacke lithofacies association. The sediments are immature, from both textural and mineralogical perspectives. Coarse-grained rocks at the base of the sequence contain primary erosional remnants of the volcanic rocks that they overlie. The coarse-grained rocks forming the base of the stratigraphic section are most likely syn deformational, proximal, debris-flow deposits, and these grade into finer-grained rocks probably representing fluvial deposition with increasing distance from the sediment source.

In general, the sediments at Royal Hill comprise a large-scale fining-upward sequence, from conglomeratic units towards the south of the deposit, to finer-grained wackes with intercalated conglomerates to the north. Poor sorting and a high level of mineralogical immaturity in the wackes and pebble conglomerate of Royal Hill probably indicate rapid sedimentation, and little reworking. Royal Hill is approximately 4.5 kilometers east of the Mayo deposit, where there is a similar type of sedimentary sequence.

III. B. 1. C. Mayo deposit conglomerate and wacke:

The stratigraphy of the Mayo deposit begins with felsic-to-intermediate-volcanic rocks, which are overlain by a fining-upward sequence of conglomerate and wacke

(Figure 3.25). The unconformity between the sedimentary and igneous rocks is inferred through characteristics of the volcanic rock in proximity to the contact: it is often washed out looking and crumbly (although not gouge), possibly indicating a period of weathering and the development of a soil horizon prior to the deposition of the sedimentary rock. The wacke is brown to greenish in hand sample, and is fine-grained and moderately sorted, with grains ranging in size form 1 millimeter to clay sized. Small-scale crossbeds, generally four to five centimeters thick, composed of magnetite and hematite, are common in the wacke and generally indicate a north-up polarity. The rock is often strongly magnetic in proximity to these beds, however this feature does not produce a noticeable anomaly in the aerial magnetic data. Beds of wacke range in thickness from 30 centimeters to several meters, and are often intercalated with coarser-grained conglomeratic beds, which are clast supported, and have grains ranging in size from approximately five to fifteen millimeters. QLF and Qm, Lt, F contents of the wacke, as determined through point counts of 200 grains from 4 thin sections are consistent with known rocks of transitional arc provenance (Figure 3.26; Dickinson, 1983).

The coarser-grained conglomeratic units of Mayo are matrix to clast-supported, and consist of 2 to 5 centimeter, subangular to subrounded clasts of porphyritic felsic volcanic clasts, mafic volcanic clasts, and felsic volcanic clasts, with minor monocrystaline quartz, feldspar, and quartzite clasts in a sericite, chlorite, carbonate, and sometimes, magnetite matrix, as revealed by petrographic analyses (Figure 3.27). Beds of conglomerate generally range in thickness from 40 centimeters to 4 meters, and are intercalated with wacke, generally found lower in the stratigraphic section of the Mayo deposit (Figure 3.25).

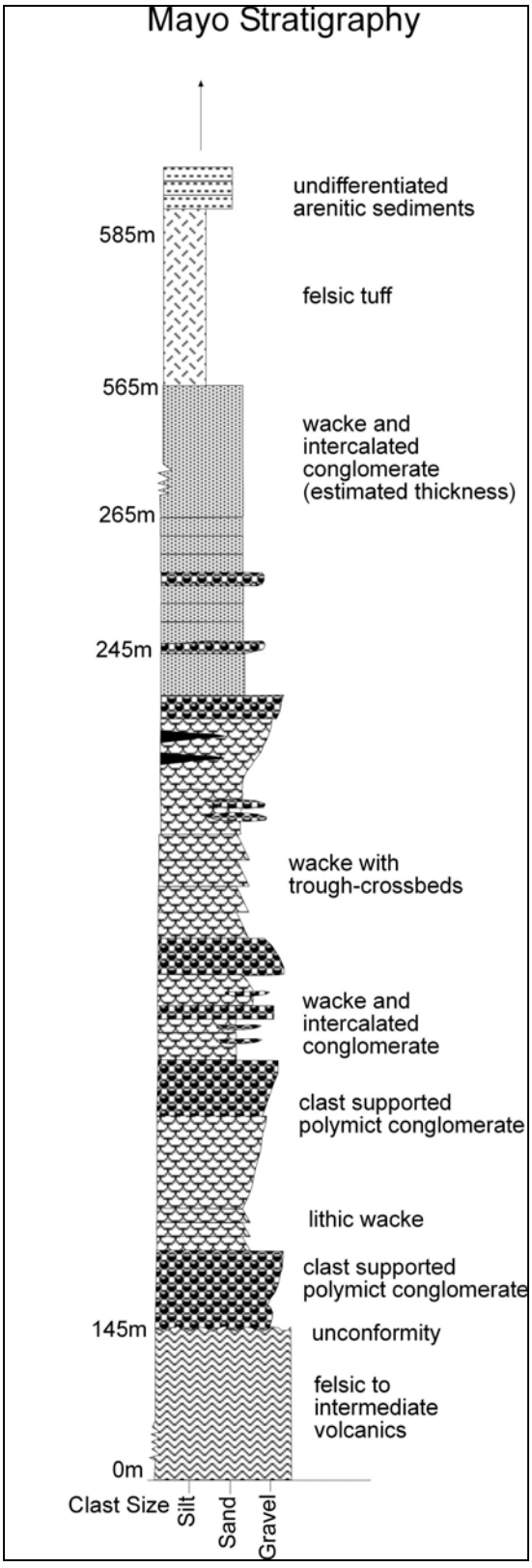

Figure 3.25: Stratigraphic column of the Mayo deposit, based on field observations, and interpretation of diamond-drill core. Sedimentary rocks unconformably overlie mafic and felsic igneous rocks, and grade upward, from course grained, clast supported conglomerate, into wacke and intercalated, finer grained, conglomerate. These sedimentary rocks later form a depositional contact with felsic tuff, which in turn contacts sandstone to the north of the Mayo deposit.

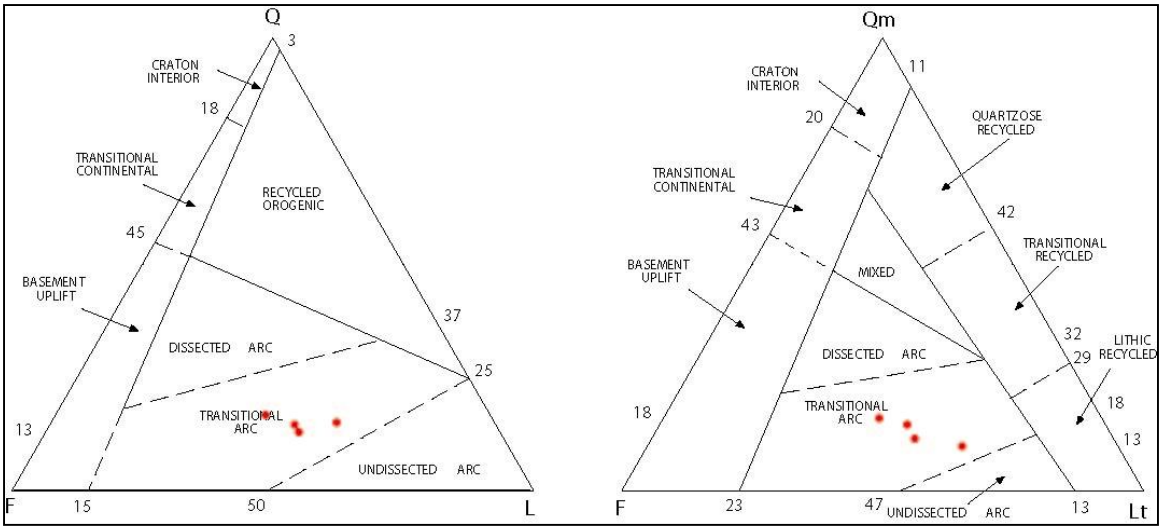

Figure 3.26: (left) Ternary diagram of quartz (Q), feldspar(F), and lithic-fragment(L) content of wacke from the Mayo deposit, consistent with transitional-arc provenance (Dickinson, 1983). (right) Ternary diagram of monocrystalline quartz (Qm), feldspar(F), and lithic-fragment(Lt) content of wacke from the Mayo deposit, also consistent with transitional arc provenance (Dickinson, 1983). Diagrams based on point-counts of 200 grains from four thin sections of wacke from the Mayo deposit.

The conglomeratic sediments of the Mayo deposit contain a higher percentage of volcanic clasts than any of the other deposits on the RGM property. The basal conglomerates are composed mainly of mafic and felsic volcanic clasts, and are thereby most likely representative of a bimodal lithofacies association, and are most similar to the polymict-breccia and conglomerate-wacke lithofacies associations (e.g. Eriksson et al., 1994) like Royal Hill, but with a slightly different sediment source.

While looking at conglomerates from various stratigraphic depths of the Mayo deposit, it seems that the overall percentage of mafic and felsic volcanic clasts decreases with time (lower strata have higher percentages of igneous clasts), and the inverse can be said for monocrystalline quartz and feldspar (Figure 3.27). Additionally, composition of the wacke tends more towards the transitional arc provenance than the undissected arc provenance. The changing composition of the conglomerates with depth, and the transitional, rather than undissected arc provenance of the sediments at Mayo indicates that the sediments were deposited in a later stage of arc-evolution than the sediments mentioned above.

III. B. 2. Recycled orogenic sedimentary rocks:

III. B. 2. A. Pay Caro conglomerate and wacke:

Volcanic rocks in the Pay Caro pit are unconformably overlain by basal conglomerate, composed of primary-erosional byproducts of the underlying-volcanic rocks. The unconformity is inferred through the presence of primary-erosional byproducts of the underlying-volcanic rock comprising a dominant clast population in the conglomerate above. The contact is a zone of ductile shearing, and mylonitized

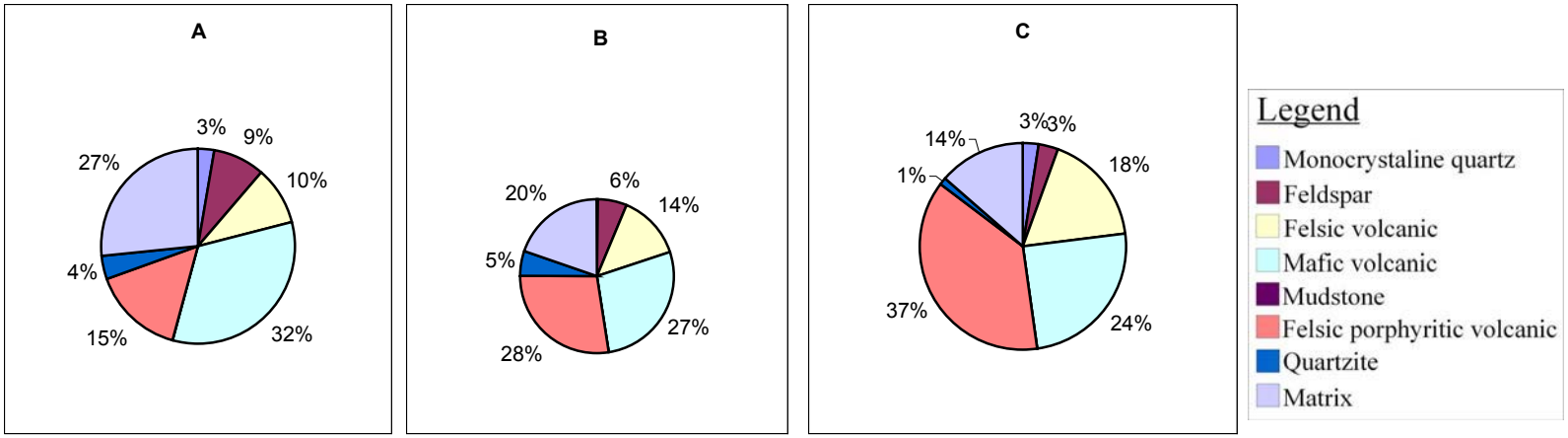

Figure 3.27: (A) Pie chart indicating clast population of the Mayo deposit conglomerate from approximately 60 meters (stratigraphic depth), based on point-counts of 200 grains from 3 thin-sections and analyses of diamond drill-core (counts of clasts per intervals of drill-core). (B) Pie chart indicating clast population of the Mayo deposit conglomerate from approximately 80 meters (stratigraphic depth), based on point-counts of 200 grains from 5 thin-sections, and analyses of diamond drill-core. (C) Pie chart indicating clast population of the Mayo deposit conglomerate from approximately 124 meters (stratigraphic depth) based on point counts of 200 grains from 2 thin sections and analyses of diamond-drill core.

conglomerate spans a zone of several meters to the south of the contact (Figure 3.28 and 3.29).

The stratigraphy of the Pay Caro deposit has been subject to the most intense analysis during this study, as the Pay Caro pit offers the best exposure of fresh rock anywhere on the RGM property. The sequence of sedimentary rock consists of 30 meters of basal conglomerate with intercalated wacke, overlain by approximately 70 meters of crossbedded wacke. Fining-upward sequences and intercalated one to three meter thick beds of conglomerate are common features in the wacke. The conglomeratic wacke grades into siltstone and mudstone with intercalated wacke that has a thickness of about 30 meters (Figure 3.30). In general, the stratigraphy of Pay Caro can be described as one large-scale fining upward sequence, with a basal conglomerate grading into wacke with intercalated pebble conglomerate, and finally, siltstone and mudstone.

The basal conglomerate forms beds 5 to 10 meters in thickness, with thin (1 meter and less) intercalations of wacke and finer-grained conglomerate. The conglomerate is clast supported, and the morphology of quartzite clasts is generally subrounded, whereas less-stable clasts are usually highly sheared and elongate, thus obscuring their original morphologies. In proximity to the contact with the volcanic rocks, the conglomerate is sheared. The sense of shear is parallel to the regional foliation (~110°), and reverse-sinistral-oblique motion is recorded by a strong stretched-pebble lineation in the mylonitized conglomerate. Evidence of shearing including cataclasis and dynamic recrystalization are observable in the field and in thin section (Figure 3.29). Field and petrographic analyses indicate that the conglomerate is composed of mainly mafic-

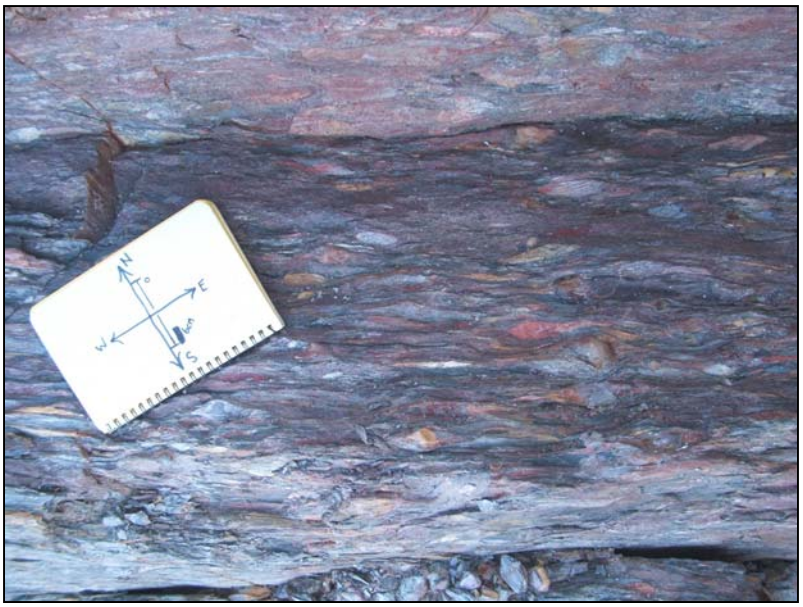

Figure 3.28: Photograph of sheared Pay-Caro basal conglomerate, along fault contact with volcanic rocks. Field-book for scale, and to show approximate orientation of shearing.

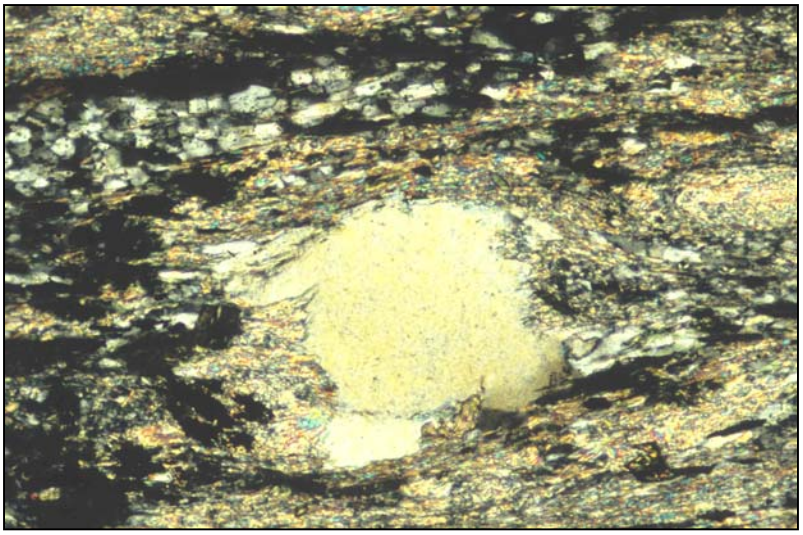

Figure 3.29: Photomicrograph of recrystalized "tail" on quartz clast (to right of large unextinct grain in center of image) - Pay Caro basal conglomerate. 100X, XPL.

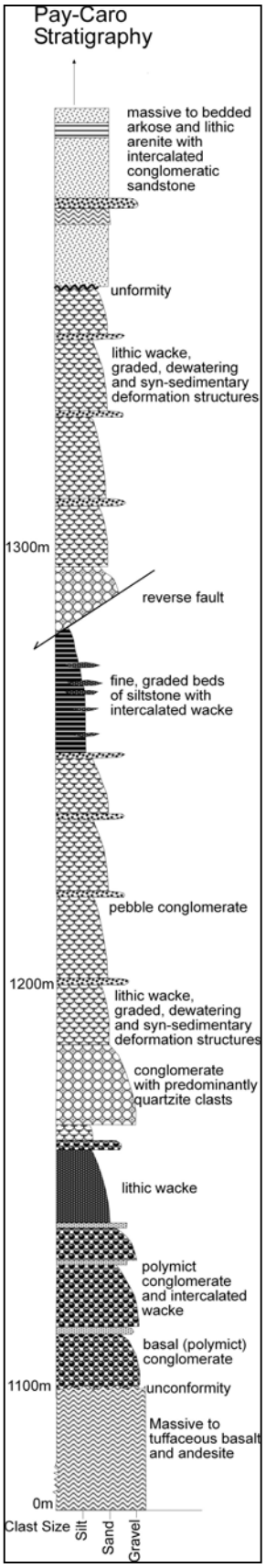

Figure 3.30: Stratigraphic column of the Pay Caro deposit. Sedimentary sequence begins with fault contact with andesitic to basaltic igneous rocks below and is comprised of basal, clast supported conglomerate that grades into lithic wacke with intercalated pebble conglomerate. The wacke and conglomerate then grades into siltstone and intercalated wacke. Conglomerate from lower in the stratigraphic section is juxtaposed on top of the siltstone through a reverse fault that runs along approximately the center of the Pay Caro pit. The wacke and conglomerate unconformably contacts arentitic sediments to the south of Pay Caro pit.

Figure 3.31: Photograph of slump structure in diamond drill-core sample of Pay Caro wacke. Core is ~4cm across.

volcanic clasts, quartzite, felsic-volcanic clasts, and to a lesser extent, feldspar and monocrystalline quartz (Figure 3.32).

The basal conglomerate grades into lithic wacke with intercalated pebble conglomerate, forming beds of approximately 2 to 4 meters in thickness. The wacke and intercalated pebble conglomerate are composed of quartzite, felsic and mafic-volcanic clasts, and monocrystalline quartz, with a quartzite, chlorite, sericite, plagioclase matrix (Figure 3.32). The wacke is gray to beige in hand sample, fine-to-medium-grained, and contains some small intervals (20 to 30 centimeters) of intercalated coarser-grained (~1 to 3 millimeter) material. Point counts of 200 grains from 11 thin sections show that the Pay Caro wacke and pebble conglomerate is of recycled-orogenic and or recycled-lithic provenance when plotted on QLF and Qm, F, Lt diagrams (Figure 3.33; Dickinson et al., 1983). Trough crossbedding and graded bedding are prevalent sedimentary structures in the Pay Caro wacke. Small crossbeds of magnetite and hematite, several centimeters in width, are common and generally indicate a south-up polarity. Soft-sediment-deformation structures including slumping and dewatering structures are also present in the wacke (Figure 3.31).

The sedimentary rocks of Pay Caro represent a continuous fining-upward sequence of about 200 meters in thickness, with conglomerate at the base, and siltstone-mudstone at the top. This is indicative of either a deepening basin, or the erosion of paleotopography, thereby decreasing the energy of stream driven erosion and deposition over time. The deepening-upward sequence, and the greater level of textural and mineralogical maturity towards the top of the sequence probably points towards a sub-aerial to shallow-marine environment, transitioning to a deeper-marine environment.

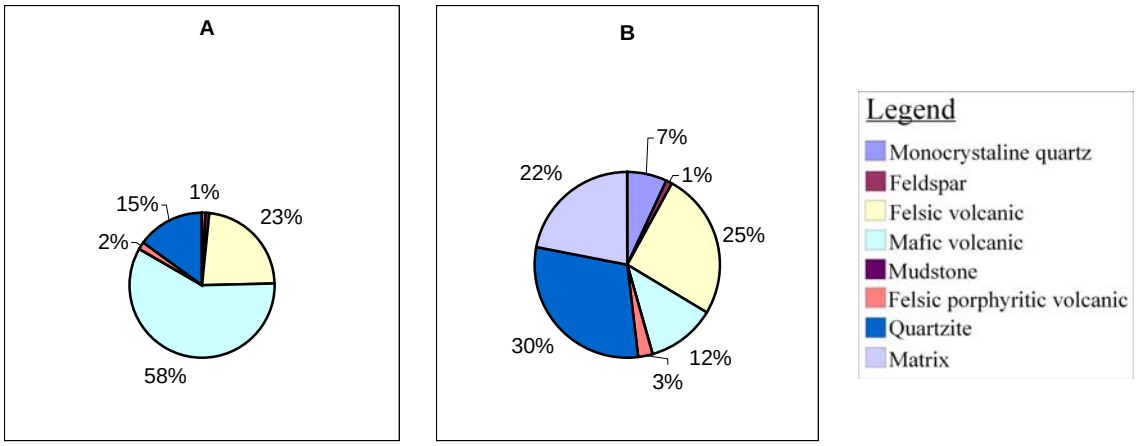

Figure 3.32: (A) Pie chart indicating clast population of the Pay Caro deposit basal conglomerate; (B) Pie-chart indicating clast population of Pay Caro conglomeratic wacke and pebble conglomerate. Based on point counts of 200 grains from 9 thin sections and analyses of diamond-drill core.

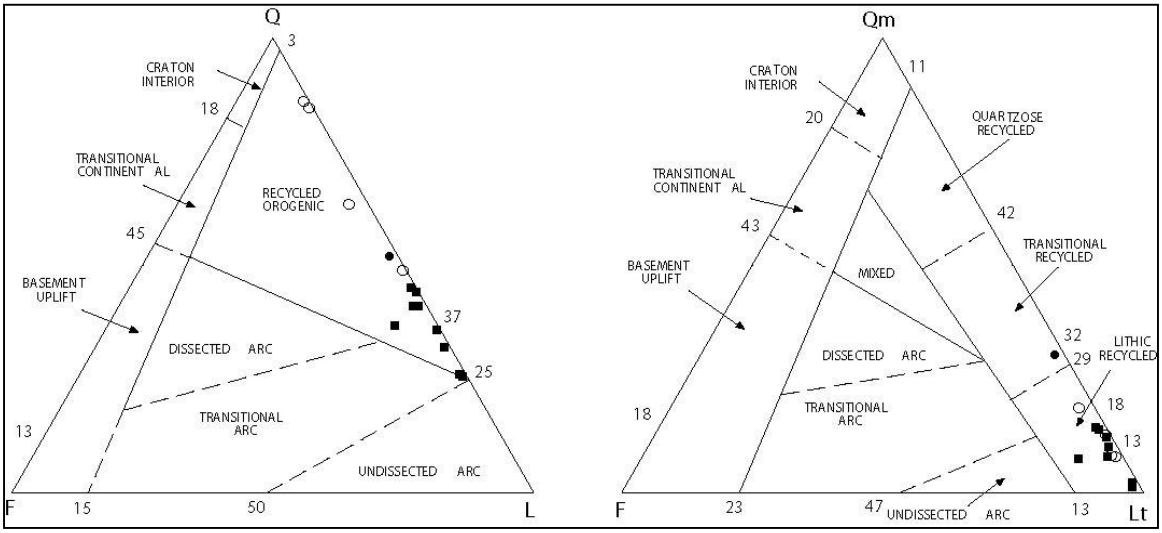

Figure 3.33: (left) Ternary diagram of quartz (Q), feldspar(F), and lithic-fragment(L) content of conglomeratic wacke and pebble conglomerate from Pay Caro deposit; consistent with undissected-arc provenance (Dickinson, 1983). (right) Ternary diagram of monocrystalline quartz (Qm), feldspar(F), and lithic-fragment(Lt) content of conglomeratic wacke and pebble conglomerate from Pay Caro deposit; also consistent with transitional arc provenance (Dickinson, 1983). Diagrams based on point counts of 200 grains from 15 thin sections of wacke from the northern side of Pay Caro pit.

This can be explained through a transition from an alluvial fan, to shoreface environment, to a shelf environment. The sediments of Pay Caro fall in between the conglomerate-quartz arenite and conglomerate-wacke lithofacies associations, as defined by Eriksson et al. (1994). However, they are of different provenance than the wackes of Mayo and Royal Hill in that they contain significantly more quartzite. This may indicate that they are erosive byproducts of pre-existing continental crust, deposited during the same deformational event in which sediments from the other, more igneous sources were being deposited.

Sedimentary rocks with high quartz contents in archaean greenstone belts, for example, in the western Slave Province (Easton, 1985; Padgham and Fyson, 1992), quartzites in the Chittradurga Greenstone belt in India (Naqvi and Rogers, 1983), and quartz-rich sandstones in the western Superior Province (Thurston and Chivers, 1990), are considered by Lowe, (1994) to represent the erosive byproducts of older, pre-greenstone crustal rocks. All of these sequences include clean, cross-stratified, quartz-rich sandstones deposited under shallow-water conditions and these are usually overlain by greenstone-belt-volcanic and immature-sedimentary sequences (Lowe, 1994). This description seems consistent with the rocks of Pay Caro, but the source area of the quartzite remains unclear.

Conversely, the sediments in Pay Caro could be related to a later phase of crustal recycling than the other sediments present at RGM. Models of crustal evolution proposed by Vanderhague et al. (1998) suggest a two-phase sequence of crustal accretion responsible for the formation of the granite-greenstone belts in French Guiana consisting of: (1) An early accretion of crustal blocks by accumulation of mantle-derived magmas

and building of calk-alkaline plutonic-volcanic complexes and tholeiitic ocean basalts, and (2) A period of recycling in a context of oblique convergence characterized by erosion and deposition of batholith-derived sediments in foreland basins. This explanation works equally as well as the erosion of an older cratonic source, but implies that the sedimentary sequence at Pay Caro must be younger than the sediments to the north and south.

III. B. 2. B. Rosebel Formation:

The sequence of conglomerate, wacke, and siltstone-mudstone of Pay Caro comprise a stratigraphic thickness of approximately 180 meters, and span a distance from the southern flank of the mafic volcanic rocks in the northwest of Pay Caro pit to approximately 60 meters northeast of the southwest perimeter of the known deposit. Here, a younger sedimentary formation, historically referred to as the Rosebel Formation, is encountered. The contact between the wackes of the Pay Caro deposit and the Rosebel Formation is abrupt, and appears to be a fault, juxtaposing the mudstone / siltstone and the more quartz rich sediments to the south. This outcrop corresponds to a northwest-southeast trending magnetic lineation in the same area.

Fresh-rock outcrop of the Rosebel Formation is exposed in the southern flank of the Pay Caro pit, and consists of massive to crossbedded, fine-to-medium-grained sandstones and conglomeratic sandstones (Figures 3.34 and 3.35). Intercalated lenses of conglomeratic sandstone generally several meters in thickness are present, and contain mainly well-rounded quartzite and mudstone clasts of 3-5 centimeters in diameter, with a subordinate population of felsic volcanic clasts. Saprolitic outcrops of the Rosebel Formation elsewhere within the RGM concession are composed of beige to yellowish,

Figure 3.34: Photograph of Rosebel Formation conglomeratic sandstone (south of Pay Caro pit). Black clasts are mainly mudstone, also present are quartzite, and felsic volcanic clasts (white). Sunglasses for scale.

Figure 3.35: Photograph of crossbedded sandstone, Rosebel Formation (south of Pay Caro pit).

coarse-to-medium grained sericitic quartz sandstone with generally less than 10% lithic fragments.

Rocks of the Rosebel Formation are more texturally and mineralogically mature than the other sediments observed at RGM, with significantly less lithic-volcanic-clastic material. In the southern flank of Pay Caro, sandstones considered to be part of the Rosebel Formation are found to contain quartzite, mudstone, monocrystalline quartz, and some felsic-volcanic fragments, in a matrix of fine-grained quartz and sericite (Figure 3.36). The grains in the rock are subrounded to rounded. Thin section analyses of this rock type indicate recycled orogenic provenance, like the rocks in the northern part of Pay Caro.

To the south of the Pay Caro deposits, spanning a distance of approximately 4 kilometers, is a flat and horizontally-stratified region of savannah (Brinck, 1955). The area spans a distance from east to west of approximately 30 kilometers. The savannah area is covered by several centimeters to 1.5 meters of alluvial material (Brinck, 1955). Little is know about the bedrock geology of this area, and diamond drilling has not been carried out by RGM, except in the case of the Rosebel gold deposit (not to be confused with the Rosebel Formation or Rosebel gold mine). However, some data exists through a reverse percussion (RC) drilling campaign, carried out by RGM for exploration purposes to the west of the Rosebel deposit. Brinck (1955), in conjunction with the geologic survey of Suriname (GMD) did some of the first drilling in the savannah area and ascertained that the basement rocks of the savannah are pale-white, creme-colored, or light brown conglomeratic sandstones, composed mainly of quartz and sericite. The rocks in the upper part of the weathering profile are very crumbly and poorly

consolidated (Brinck, 1955). The conglomeratic parts of the rock consist of quartzite bands and lenses, oriented parallel to the schistosity of the rock (Brinck, 1955). Quartz veins cut these rocks, and therefore, they are not of recent formation, but are weathering products of the bedrock below (Brinck, 1955).

Core drilling carried out by the GMD reveals that the saprolite horizon of the Savannah area continues to a depth of approximately 14 meters (Brinck, 1955). Fresh rock from below is a gray, fine-to-medium-grained, schistose, conglomeratic sandstone (Brinck, 1955). Petrographic research reveals that the mineralogical composition of these rocks deviates from the other sedimentary rocks to the north and south (Brinck, 1955). These rocks are chlorite and calcite containing, epidote-sericite-albite-quartz schists (Brinck, 1955).

Gross mineralogical composition of these rocks, determined by Brinck (1955), consists of 40-50% quartz, 20-30% plagioclase, 13% sericite, 14% epidote, and 1% chlorite. Accessory minerals include rutile, titanite, garnet, and tourmaline (Brinck, 1955). This composition is more or less consistent with my own petrographic analyses of rocks of the Rosebel Formation near the Rosebel deposit (Figure 3.36) and south of the Pay Caro deposit. The stratigraphic thickness of the Rosebel Formation at RGM is unknown.

Brinck (1955) made the argument, based on secondary alteration minerals, that the bedrock of the savannah area is the same as the rock of the Armina / Orapu Formations, but has been altered due to the intrusion of a theoretical granitic intrusive below. However, this argument is refuted by data obtained through reverse percussion drilling, carried out by RGM during 2005. Lithologies consistent with the Armina

Group, including volcaniclastic and volcanic rocks were encountered at a shallow depth below alluvial material in the central trend to the west of the Rosebel deposit. Therefore, it is surmised that a similar sequence of arc-related sedimentary rock, and volcanic rock, as is encountered at the other gold deposits on the concession is probably present below the Rosebel Group along the central trend. However, detailed stratigraphic information was not obtained through RC drilling, due to the nature of that type of drilling (samples obtained through RC drilling are typically either rock powder, or fine chips, and this material is sometimes difficult to interpret, although general rock types can be distinguished). The Rosebel gold deposit is located to the east of the savannah area, and is situated in the eastern part of the savannah area and is discussed below.

Rosebel Deposit:

The most enigmatic gold deposit on the RGM concession is the Rosebel deposit, as unlike the other deposits, the Rosebel deposit does not seem to be associated with a contact between volcanic and sedimentary rocks. Located within the boundary of the aforementioned savannah area, the deposit is situated along a narrow magnetic anomaly that trends parallel to the regional foliation (110°). The deposit was originally thought to be related to the so called "south trend" of mineralization, which includes the Royal Hill and Mayo deposits, but this does not appear to be the case in the magnetic data, as it appears to be located along a different magnetic trend (Plate 3).

To the north of the Rosebel deposit, a gray, fine-to-medium grained sandstone spans a swath of ground approximately 1.7 kilometers to the north, where it is in contact with sediments of the Armina Group. To the south of the Rosebel deposit, clast-supported pebble conglomerate forms a band approximately 7 meters in thickness. This

conglomerate is composed of quartzite, feldspar, and monocrystalline quartz, with ~5% volcanic clasts and ~15% matrix (Figure 3.36). QLF and Qm, Lt, F diagrams (after Dickinson, 1983) of sandstones south of the Rosebel deposit indicate that they are either of the recycled orogenic or transitional arc categories respectively, although the former is probably the correct interpretation based on the comparatively high quartzite-clast content that drags the data into the transitional arc category on the Qm,F,Lt diagram (Figure 3.37).

The composition of the sedimentary rocks of the Rosebel deposit is different than any of the other deposits on the RGM property, with clasts of mostly quartzite, monocrystaline quartz, and feldspar. Unlike any other deposit, the Rosebel deposit does not seem to be associated with any Proterozoic volcanic rocks, although the dikes may play an influential role in gold mineralization at Rosebel. The sedimentary rocks at the Rosebel deposit are of recycled orogenic provenance, and the rock also contains more feldspar than most of the other rocks at RGM. Therefore, the sediments at the Rosebel deposit, like those of Pay Caro either represent a later phase of sedimentation, or a different sediment source during deposition.

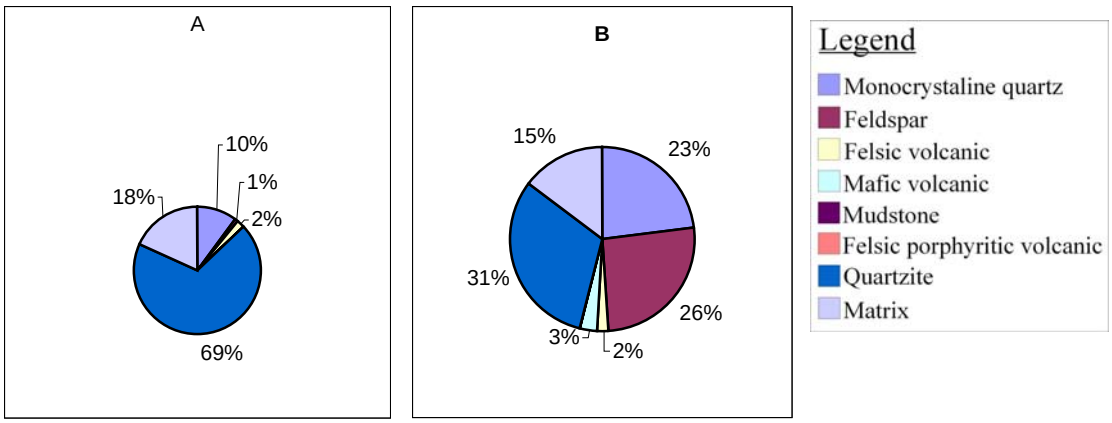

Figure 3.36: (A) Pie chart indicating the clast population of the conglomeratic sandstone to the south of the Pay Caro pit, based on point-counts of 200 grains from 5 thin sections, and field observations. (B) Pie chart indicating the clast population of conglomerate from the Rosebel gold deposit, based on point counts of 200 grains from 4 thin sections. Note subordinate presence of volcanic material in contrast to most other sedimentary rocks in this study.

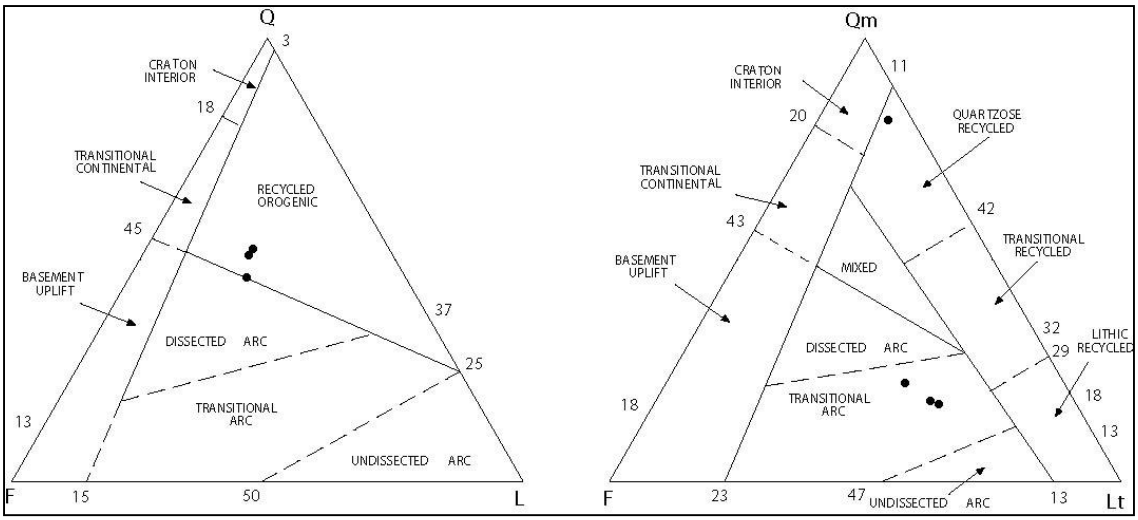

Figure 3.37: (left) Ternary diagram of quartz (Q), feldspar(F), and lithic fragment(L) content of conglomeratic sandstone from the Rosebel deposit; consistent with recycled orogenic provenance (Dickinson, 1983). (right) Ternary diagram of monocrystalline quartz (Qm), feldspar(F), and lithic-fragment(Lt) content of conglomeratic sandstone from the Rosebel deposit; consistent with transitional arc provenance (Based on Dickinson, 1983). Comparitively high quartzite content of this rock drags the points down into the transitional arc category when the quartz is grouped with the lithic fragments (diagram on right). Therefore the provenance is more likely recycled orogenic than transitional arc. Diagrams based on point-counts of 200 grains from 4 thin sections of conglomeratic sandstone from the Rosebel deposit.

III C. Felsic plutonic rocks - "Brinck's Granite:"

Approximately 2 kilometers south of Royal Hill, and 2.2 kilometers southwest of Mayo is a granitic body with a radius of about 7 kilometers (Plate 1). Field observations of the contact between the granite and the country rock indicate that it is not a fault, because the contact is not sheared, and there is no evidence of displacement. However, whether or not there is a contact aureole of metamorphism in the wall rock proximal to the granite is not clear in the field because of intense weathering. The age of the granite in comparison to the other sedimentary and volcanic rocks discussed previously is not certain. However, given the intense metasomatic alteration in the Royal Hill rocks just north of the granite, and the low potassium feldspar content of the conglomerates and wackes of the undissected arc related sediments, it is likely that the granite post dates the deposition of most of these sediments, and therefore also intrudes the underlying volcanic rock.

Quartz veins observed in country rock proximal to the granite are associated with a deformational event and the veins do not cut the granite-country rock contact. The granite, therefore, must post-date at least this deformational event. There are no mineralized quartz veins found within the granite itself, but there are mineralized quartz veins in the country rock adjacent to the granite. Magnetic patterns in the country rock next to the granite appear to bend around the granite body, reflecting either warping of the units around the granite during tectonism, or possibly doming during the intrusion of the granite (Cambior, 2003).

Brinck (1955) carried out some of the first petrographic work on the granite, hence the name "Brinck's granite." The granite is medium grained, with crystals typically

about 2-4 millimeters, and contains less than 10% mica; hence it is classified as aplite (Brinck, 1955). In thin section, undulate extinction of quartz grains, and sausseritization of plagioclase crystals are common phenomena. Chlorite and minor epidote commonly fill fractures between grains. Inclusions of apatite and zircon in the plagioclase are commonly present (Figures 3.38 and 3.39). Some zircons in the granite show rounded, highly metamict cores, and zoned overgrowths.

The granite is peraluminous. A plot of REE's normalized to chondrites (Figure 3.40 Sun and McDonough, 1989) show a pattern consistent with CA2-type Archaean calc-alkaline plutons, which have lower rare-earth-element concentrations than do CA1-type plutons, are relatively small plutons, and are thought to originate from lower crustal depths (Sylvester, 1994). The granite is enriched in incompatible elements in comparison to the other igneous rocks at RGM, indicating that it was probably of a later crystallization age than the other igneous rocks.

Brinck's granite probably represents the most advanced phase of magmatic evolution present at RGM. It is peraluminous, is enriched in incompatible REE's, and has the most calk-alkaline affinity of all the rocks at RGM. Felsic clastic material at the Mayo deposit, which is also probably late-phase, has a similar pattern of REE distribution to that of Brinck's granite. The granite and the felsic rocks of Mayo are also geographically close to one another (~ 3 kilometers apart), so there may be a link between the felsic igneous rocks of Mayo, but more data is required to assess this assertion.

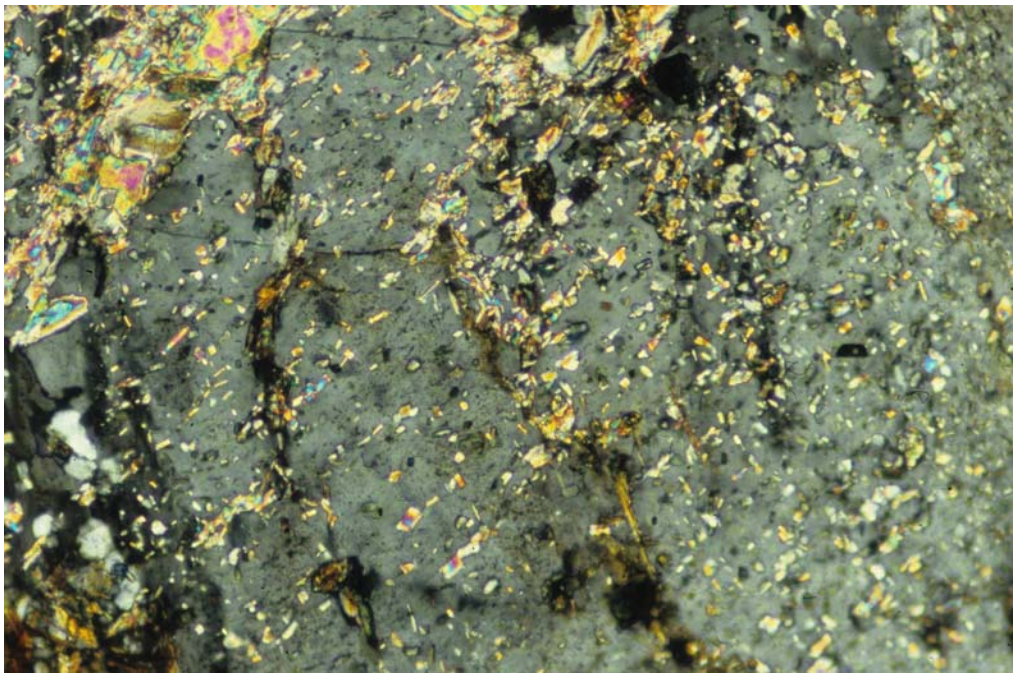

Figure 3.38: Photomicrograph of a sausseritized plagioclase crystal from "Brinck's Granite." Note sericite along twinning planes. 100X, XPL.

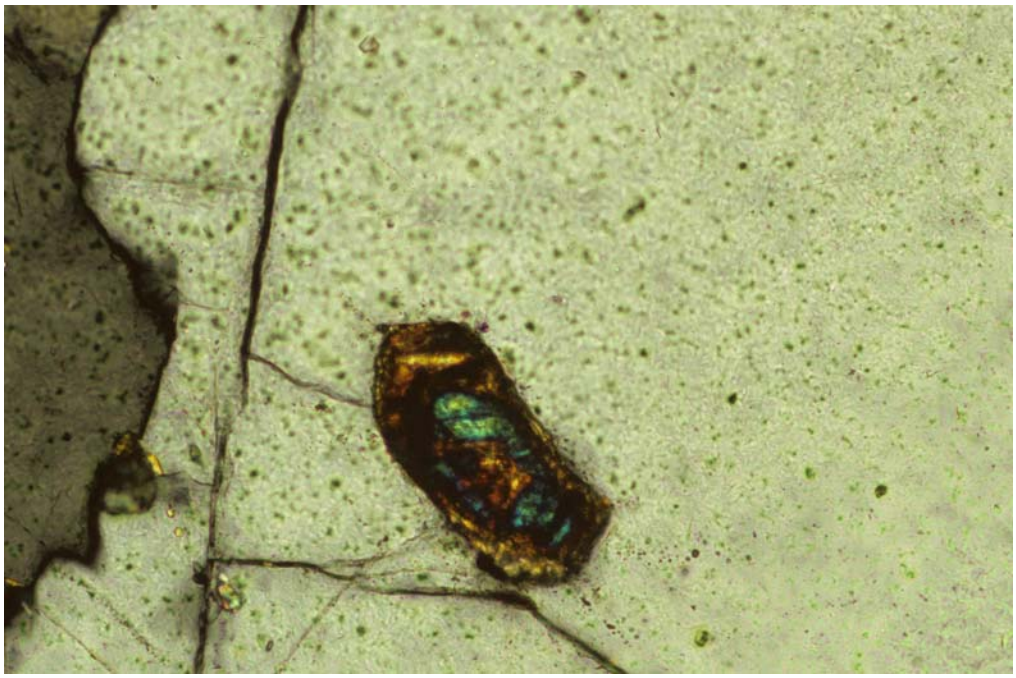

Figure 3.39: Photomicrograph of a zircon included in plagioclase from "Brinck's Granite." Note inherited core with higher order interference color. 200X, XPL.

Sedimentary rocks of dissected arc provenance have not been identified at RGM. It can therefore be surmised that the granite did not contribute a significant amount of sediment to the depositional environments at RGM during most of the Transamazonian orogeny, due to low feldspar contents in most of the sedimentary rocks. However, there is more feldspar in the sedimentary rocks of the Mayo deposit than in any of the other sediments at RGM, and they are of transitional arc provenance. This may also support the link between the rocks of the Mayo deposit and the granite, mentioned above.

III D. Mafic dikes of the Rosebel deposit:

Unlike any of the other deposits on the RGM property, there are no known Proterozoic igneous rocks in proximity to the Rosebel deposit (Figure 3.41). A series of three, north-south oriented, diabase dikes intrudes the country rock to the west of the Rosebel deposit, and are speculated to be Mesozoic in age (Brinck, 1955). Petrographic analyses of these rocks indicate that they are unaltered and less weathered than other rocks of RGM, with twinned, un-sausseritized plagioclase crystals, and augite visible in thin section (Figure 24). The dikes are also undeformed. These observations indicate that they are probably younger than other RGM rocks.

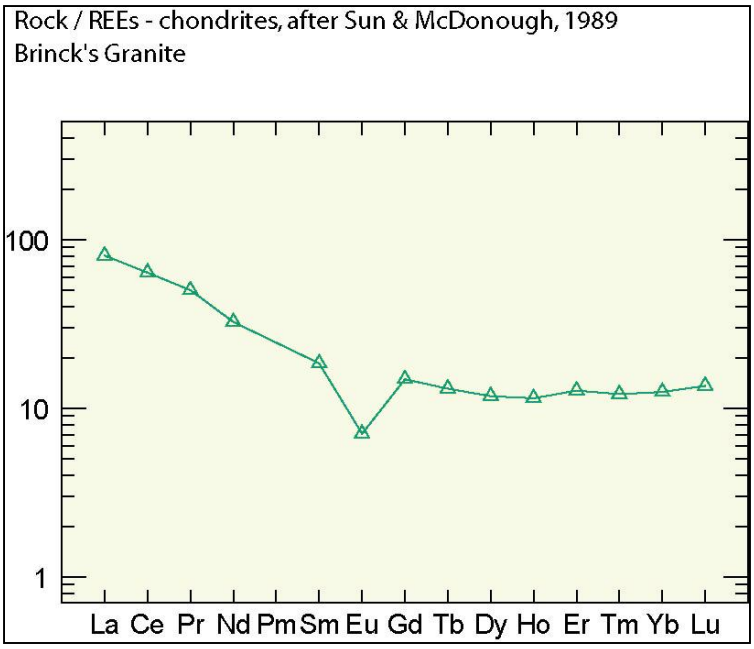

Figure 3.40: REE diagram for Brinck's Granite, normalized to chondrites, after Sun & McDonough, (1989). Note enrichment in incompatible REE's and negative Eu anomaly, common in leucogranites.

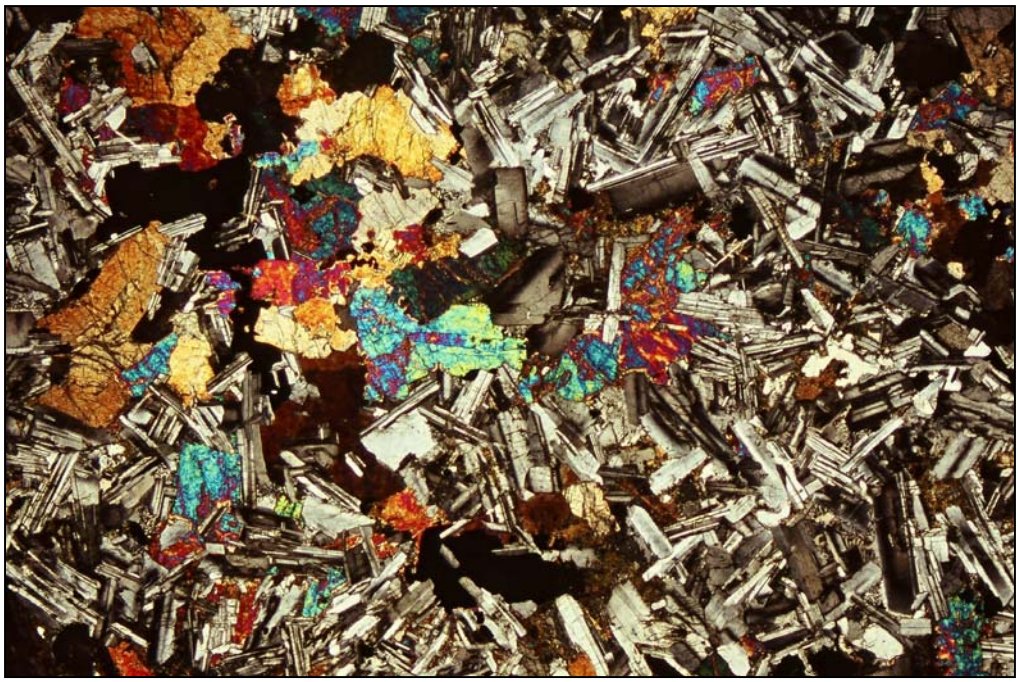

Figure 3.41: Photomicrograph of diabase dike proximal to Rosebel deposit. Note unaltered plagioclase crystals with polysynthetic twinning, and augite crystals (higher order interference colors). 20X, XPL.

IV. Structural geology and metamorphism:

The structure of the RGM property resembles a synclinorium, about 30 kilometers wide, and trending 110°. The northern limb of the synclinorium is delineated by the hill-forming rocks of the north trend, and the southern limb is thought to be delineated by the hill-forming rocks of Brownsberg, approximately 18 kilometers southwest of the RGM property (Brinck, 1955). The geometry of the rocks at RGM is indicative of at least three episodes of deformation, reflecting a changing stress regime during the Transamazonian Orogeny, resulting in folds, refolded folds, faulted folds, and folded faults. Most commonly, the rocks are isoclinally folded, with axial surfaces of folds striking parallel to the regional foliation (110°).

There are also three different orientations of quartz veins found at RGM that reflect the multi-deformational history of the rocks. Early veins are deformed and sometimes cut by later vein sets (Cambior, 2003). Gold deposition at RGM is directly related to the quartz veins. The quartz veins range in thickness from less than one centimeter to two meters, and are most prevalent in areas of rheological contrast, especially near the contacts between sedimentary and volcanic rocks. Gold occurs as individual crystals within veins, and as inclusions in pyrite crystals in vein selvages. Metasomatic alteration associated with the quartz veins varies from the north to the south of the RGM concession. In the north, the veins are more often associated with a potassic alteration, whereas in the south they are more often associated with tourmaline and

carbonate alteration. The tourmaline alteration may be related to the intrusion of the granite (Brinck, 1955; Cambior, 2003). All of the rocks at RGM, with the exception of the mafic dikes, have been metamorphosed to low-to-mid-greenschist facies. Minerals such as chlorite, sericite, epidote, carbonate, tourmaline, chloritoid, and in some cases andalusite, are secondary minerals in the RGM rocks. Structural deformation and metasomatic alteration vary from deposit to deposit, and are discussed below.

IV. A. North-trend rocks:

The rock units of the north trend generally strike 110°, dip nearly vertically, and appear to conformably contact one another. Bedding and foliation are generally parallel in the north trend rocks, the obvious exception being in fold hinges. Chlorite and sericite, associated with greenschist-grade metamorphism define the foliation, as observed in thin section.

Tight, isoclinal folds, with widths of several to tens of centimeters are present in the mudstone, and folds of greater widths are present in the wacke. Transposed and boudinaged bedding are common features in the mudstone. Folding in the conglomerate appears to be relatively broad, with folds of up to 40 meters in width. A series of several isoclinal folds of widths between about 200 and 400 meters have been identified during field mapping in the north trend (Plates 1, 2, and 3). Hinges of these folds generally trend around 280°, parallel to the regional foliation, and plunge moderately to the west (Figure 4.1). Two episodes of folding are evident in these units and are distinguished through the presence of different hinge orientations of folds. Exhumed fold hinges of relatively small folds found in the mudstone and wacke trend 108° and plunge 74 and trend 295° and plunge 4°. The steeply plunging folds are more common than the subhorizontal folds.

The highly folded geometry of the north-trend rocks is evident in not only the field, but also in aerial magnetic data (Plate 3).

Topographic and geomagnetic evidence indicate the presence of a major fault that juxtaposes the north-trend-sedimentary rocks with mafic-igneous rocks to the south (Plates 1, 2, 3, and 4). The inferred fault lies along a major topographic depression, trending roughly 110°, which is parallel to a strong-magnetic break identified in aerial-geomagnetic survey data. Based on the relative ages of the igneous and sedimentary rocks, I interpret the structure to be a steeply north-dipping reverse fault, or vertical fault that juxtaposes younger sediments of the north-trend with older volcanic rocks that lie to the north of Pay Caro.

IV. B. Pay Caro Deposits:

The contact between the volcanic rocks in the north of the Pay Caro deposit, and the sedimentary rocks to the south lies along a sinistral oblique reverse fault. This contact has been observed in fresh rock in the mine pits, and has been extensively drilled. Basal conglomerate along this contact is mylonitized, indicating ductile deformation. Schistosity of the phyllitic clasts is parallel to the direction of shortening, and this is parallel to regional foliation.

Like the rocks of the north trend, the rocks of Pay Caro and East Pay Caro have all been isoclinally folded, with fold hinges trending parallel to the regional foliation (285°), and plunging moderately to the west (Figure 4.2). Mudstone and siltstone in the southern part of Pay Caro is folded similarly to the mudstones of the north trend, with steep isoclinal folds, the axial traces of which are parallel to the regional foliation (110°). The coarser grained rocks in the north of the Pay Caro deposit are dominated by an

Figure 4.1: Equal area plot of poles to bedding from folded strata of Spin zone area. Cylindrical best fit indicates probable orientation of anticline observed in the field (260°, 64.5°)

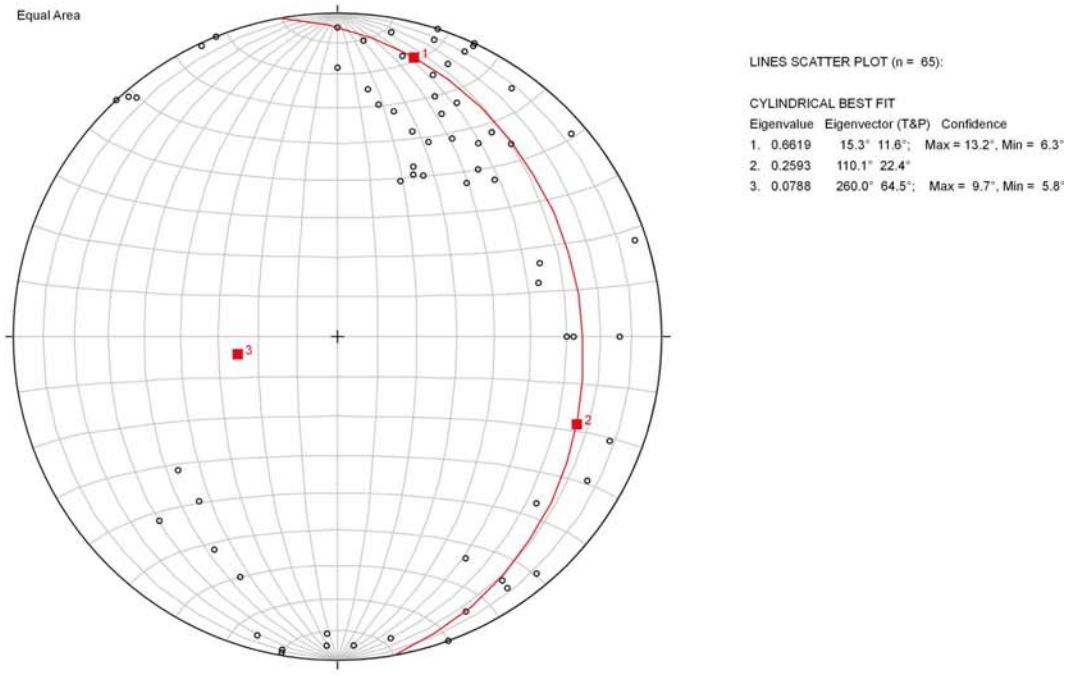

Figure 4.2: Equal area plot of poles to bedding from folded strata of Pay Caro area. Cylindrical best fit indicates probable orientation of anticline observed in the field (283°, 19°)

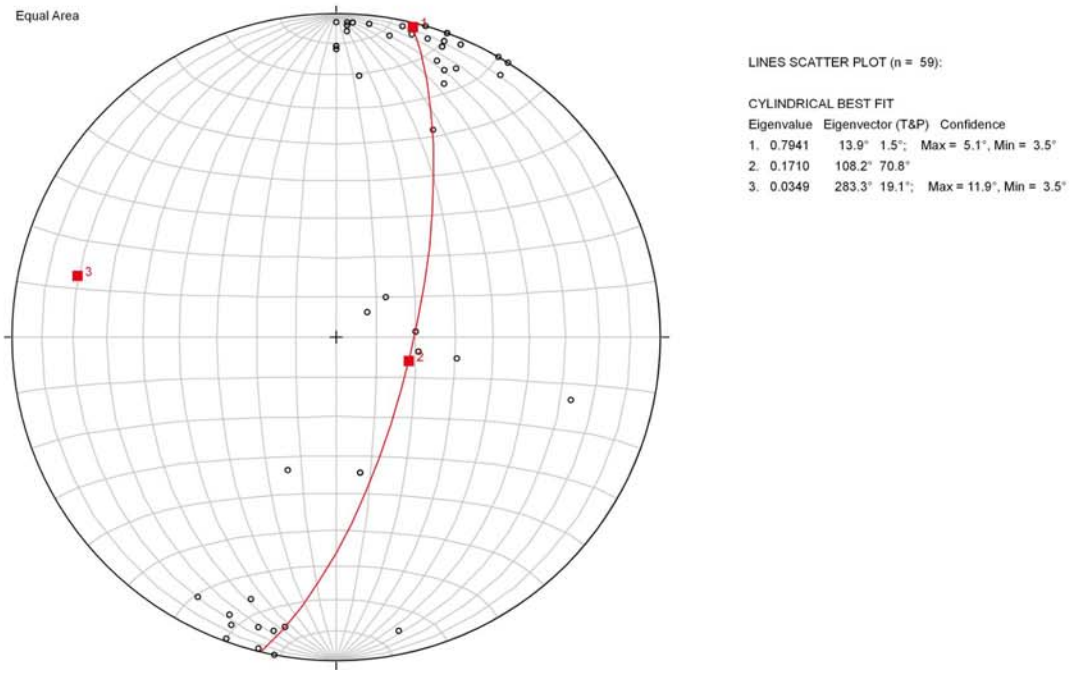

anticline-syncline structure that repeats the conglomeratic unit present in the northern part of the mine pit. This has been observed in drill core and in the field. Observed fold widths in the sedimentary rocks of Pay Caro range from 20 centimeters to 100 meters. Smaller, parasitic folds along the flanks of the larger structures are present in the wackes and mudstones, observed in the southern part of the Pay Caro pit, and have axial planes striking parallel to the regional foliation, as do the large-scale folds (Plate 4).

A reverse fault, striking 110° and dipping steeply to the north cuts across the Pay Caro pit and puts older sediments on younger sediments. Based on the estimated stratigraphic thickness repeated by the fault, the displacement is on the order of 100 meters. A sinistral strike slip fault, striking approximately 55° and dipping nearly vertically truncates the lithologies to the south of Pay Caro pit, and offsets the volcanic unit to the north of Pay Caro by at least 550 meters to the north of East Pay Caro.

Like all the rocks mentioned so far, the rocks of Pay Caro and East Pay Caro have been metamorphosed to low-to-mid greenschist grade. Plagioclase clasts in the sedimentary rocks are typically sausseritized. Chlorite and epidote are common secondary minerals. Carbonates do not have a significant presence in the Pay Caro rocks as in the Royal Hill and Mayo rocks. Also, tourmaline is a much less common alteration mineral in Pay Caro than in the rocks of the southern part of the RGM property.

IV C. South trend

The rocks of Royal Hill are the most metasomatically altered of all the rocks on the RGM property, and are also covered by the thickest saprolite horizon. Plagioclase in the Royal Hill rocks is heavily sausseritized, and carbonate, chlorite, epidote, and tourmaline are common secondary metamorphic minerals in the sedimentary rocks.

Unlike the rocks in the north trend, calcite is a prevalent secondary mineral in the rocks of Royal Hill.

Due to dense vegetation and the thick saprolite profile of the Royal Hill deposit, most of what is known about the structure of the deposit comes from diamond drilling. The structural geology of Royal Hill is not entirely clear, however small-scale-isoclinal folds of approximately 20 to 30 centimeters in width are visible in drill core of both the wacke and the arkosic sandstone of the Royal Hill area, and aerial-geomagnetic data indicates the presence of several larger (~260 meter wide) fold structures in the northern part of the deposit (Plate 3).

The Royal Hill deposit is situated between two faults, and is in an area of intense shearing. The shearing is most notable in the conglomeratic units, that contain stretched and mylonitic clasts, similar to the conglomerate in Pay Caro, but not quite as sheared. A reverse fault juxtaposes the rocks of Royal Hill with the younger-sedimentary rocks of the Rosebel Formation to the north of the deposit, and a reverse fault of less certain orientation juxtaposes the Royal Hill rocks with volcanic rocks to the south of the deposit. This contact is not well understood, but it is probably a sheared contact, similar to the contact between the conglomerates of Pay Caro and the volcanic rocks to the north, based on the similar deformation and orientation of clasts in the conglomerates towards the base of the sedimentary rocks of Royal Hill. The Royal Hill deposit seems to be along strike with the Mayo deposit, although the volcanic rocks of the two deposits are of different provenance, indicating either tectonic juxtaposition, or a difference in styles of volcanism. The Mayo sedimentary rocks are also significantly less deformed than the Royal Hill rocks, which is probably an argument for the former scenario.

Mayo

Of all the deposits on the RGM property, the rocks of the Mayo deposit seem to be the least-structurally deformed. Isoclinal folding is not evident in the rocks of Mayo. However, there is drill-core evidence that the sedimentary and volcanic rocks in the Mayo deposit are folded into a broad, east-west trending syncline-anticline structure of a width of approximately 400 meters. This interpretation is consistent with patterns visible in ground and aerial-magnetic data (Plate 4). Small-scale, north-south-oriented, strike-slip faults generally having displacements on the order of tens of meters are another prevalent-structural feature observed in the sedimentary rocks of the Mayo deposit.

The presence of folds with different orientations, steeply oriented faults, faulted folds, folded faults, and juxtaposition of different lithologies supports the argument for multiple episodes of deformation affecting the rocks at RGM, and are evidence for a structural history that is similar to that of Paleoproterozoic rocks found in French Guiana, and in other circum-South Atlantic provinces that were involved in the Transamazonian orogeny. Rocks of the Rosebel and Armina Groups in French Guiana have similar structural features to the rocks at RGM described above. In the Orapu sedimentary basin, rocks that may be equivalents to the turbiditic rocks at RGM are isoclinally folded (Vanderhague et al., 1998). The bedding of these rocks is transposed by a first schistosity, associated with the crystallization of muscovite, biotite, and chlorite, which is axial planar to macroscopic isoclinal folds (Vanderhague et al., 1998). The S_{0-1} foliation is affected by upright chevron folds which form synclines and anticlines on the order of several kilometers, axial planes of which are delineated by a second crenulation schistosity S_2, associated with the crystallization of biotite, chlorite, or sericite

(Vanderhague et al., 1998). This seems to be a very similar description to the rocks in the north trend, which are affected by tight isoclinal folds, and broader folds.

The structural evolution of the RGM rocks is possibly analogous to that of rocks of the Birimian terrane in West Africa, that were a likely counterpart to the rocks of the Guiana Shield during the Transamazonian orogeny. The present structure of the Birimian rocks reflects the three main Eburnean tectono-metamorphic phases (D_1-D_3). The first phase (D_1) resulted from a major diachronous collision, between 2150 and 2100 Ma, and was responsible for thrusting Early Proterozoic formations over the Archaean basement (Marcoux and Milési, 1993). The second phase (D_2) gave rise to large southerly striking left-lateral shear zones accompanied by emplacement of multiple granite intrusions (Marcoux and Milési, 1993). The third phase (D_3) is responsible for the north-northeasterly striking right-lateral shear zones, well marked in Burkino Faso and Niger (Marcoux and Milési 1993). The two phases of tectonic shearing (D_2 and D_3) are diachronous between 2080 and 1949 Ma (Marcoux and Milési, 1993). The D_1, D_2, and D_3 phases of deformation mentioned above seem consistent with the structural development of the RGM rocks.

V. Discussion:

The rocks at RGM represent different types of volcanism and sedimentation attributable to changing volcanism, and the development of different depositional environments during the Paleoproterozoic. Igneous rocks range from mafic to felsic, and show tholeiitic to calk alkaline affinities. The tholeiitic rocks show REE patterns similar to those of other Paleoproterozoic volcanic arcs (e.g. Wang et al., 2004), and the intermediate to felsic rocks have REE distributions consistent with island arcs as well.

Sedimentary rocks from pelagic environments, shallow marine environments, and fluvial environments are found in different locations throughout the concession, and have been tectonically juxtaposed. These rocks range in provenance from undissected arc to transitional arc, to recycled orogenic. In general, sedimentary units that are stratigraphically lower consist of conglomerates and wackes, and grade upwards into finer grained units. These are correlative sequences (Figure 5.1), and represent primary erosion in a fold and thrust belt that probably formed early on in the Transamazonian orogeny (Figure 5.2). The provenance of the lower rocks range from undissected arc, to recycled orogenic. This is probably reflective of contemporaneous erosion of different source material.

A unique and not obviously correlative rock sequence is present in the turbidites of the north-trend, and this probably represents an earlier phase of deposition in a pelagic environment, that was later juxtaposed with the younger rocks to the south, through

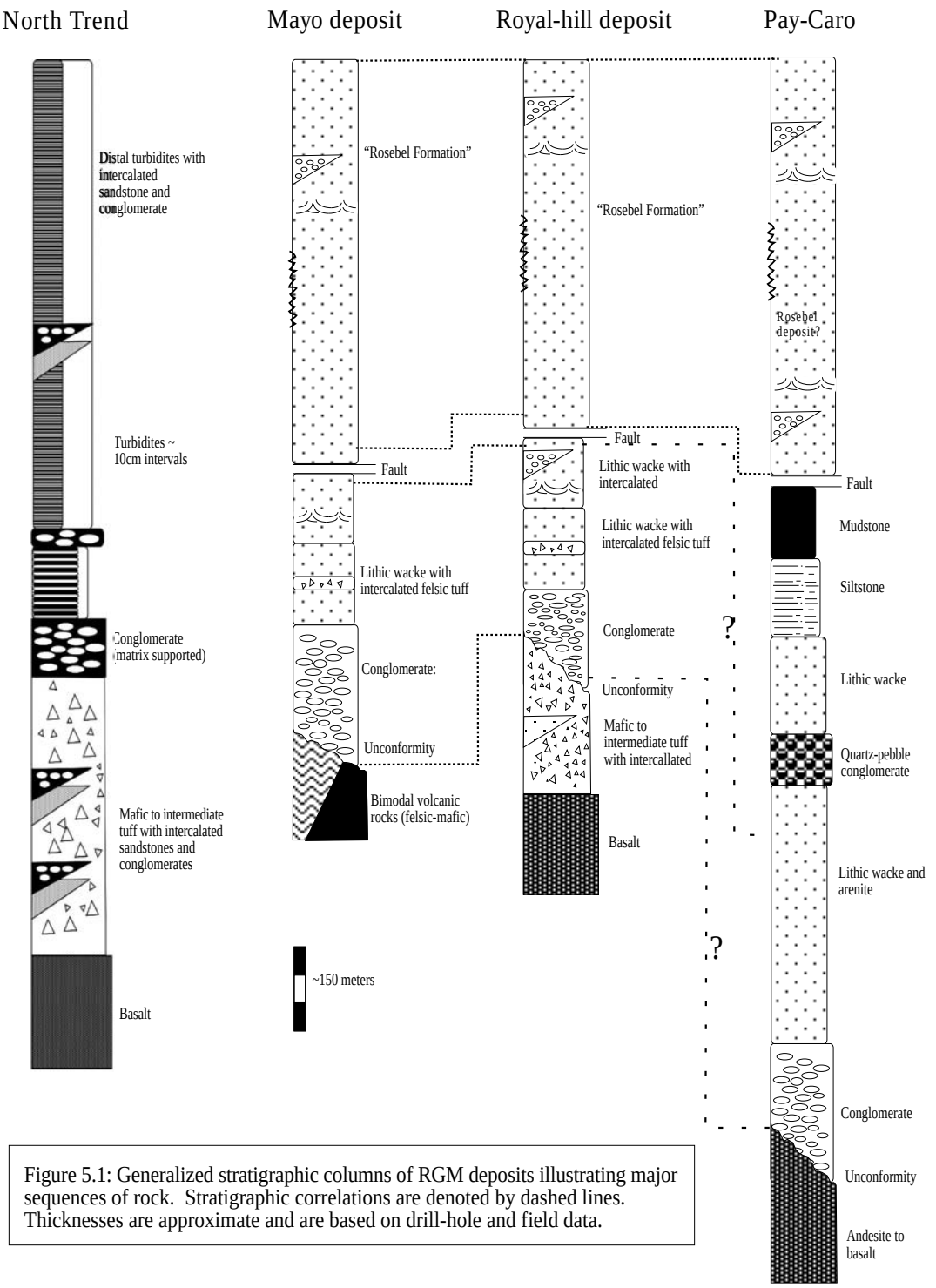

Figure 5.1: Generalized stratigraphic columns of RGM deposits illustrating major sequences of rock. Stratigraphic correlations are denoted by dashed lines. Thicknesses are approximate and are based on drill-hole and field data.

Model of Transamazonian crustal evolution

Figure 5.2: Model of crustal evolution during the Transamazonian orogeny (2.1 to 1.9 GA). The following sequence of events is depicted in the illustration, Modified in part from Delor et al., (2003).

1) North-south oriented compression between Archaean West African and South American cratons. Formation of island arc systems. Mafic to intermediate volcanism, Deposition of deep-marine sediments.

2)Intermediate to felsic volcanism with further development of island arc systems, continuationi of subduction and southern movement of island arc systems.

3) Development of thrust faults, and accretion of island arcs and associated sediments. Low angle folding, erosion - giving rise to the conglomerates of the Mayo and Royal hill deposits. Provenance is determined by local differences in eroding material.

4) Sinistral wrenching between the West African and South American cratons, steepening of shallowly dipping thrust-faults, isoclinal folding, and development of regional foliation. Development of leucogranites, and unroofing of older granodiorites.

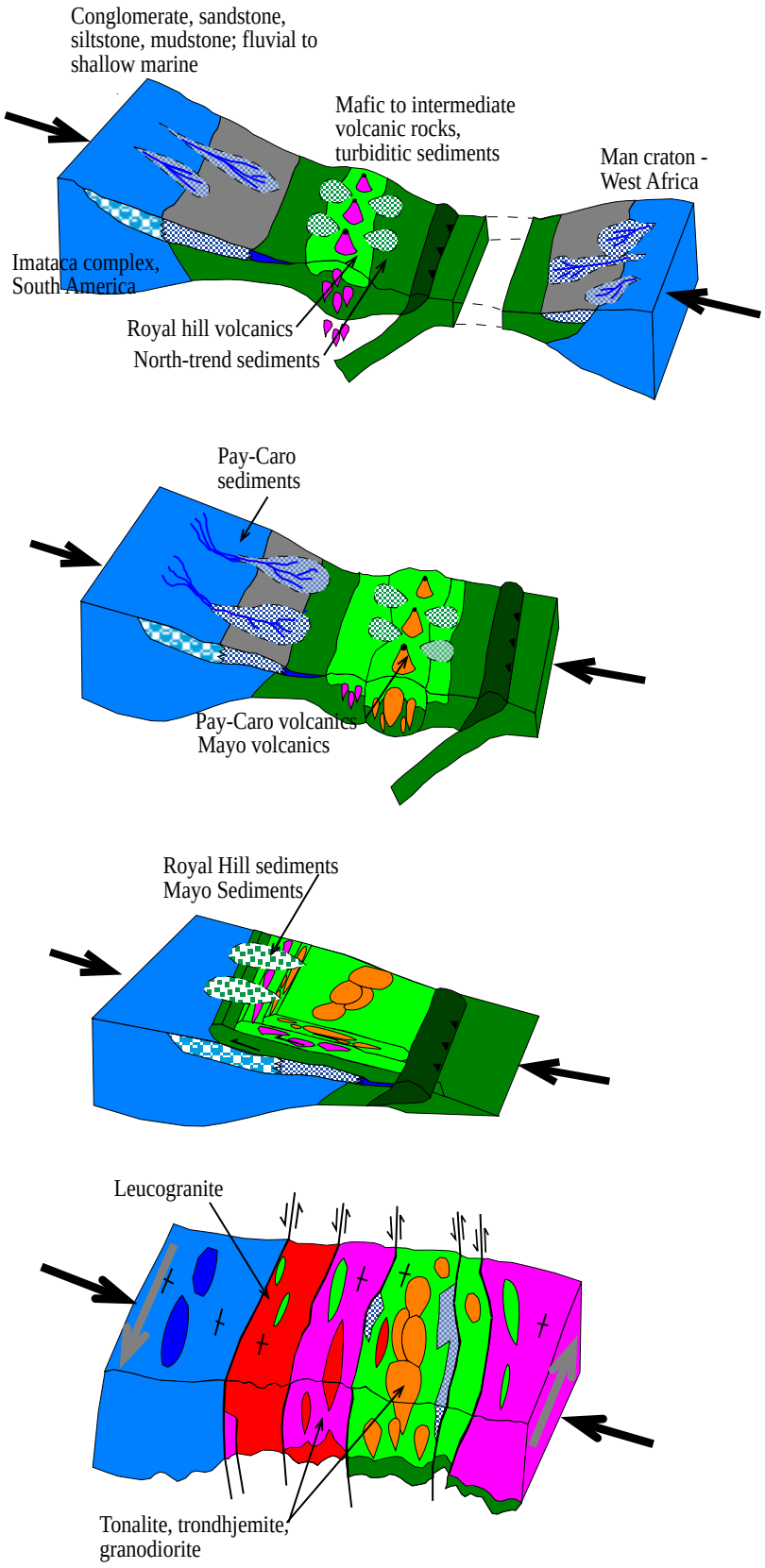

thrusting (Figure 5.2). In general, the sequence of rocks at RGM consists of mafic to felsic igneous rocks comprising the base of the stratigraphy, and this is overlain by turbiditic rocks, and partly by basal conglomerates and wackes (Figure 5.3). The sequence most likely represents: (1) The formation of an island arc system, related to the convergence of the West African and South American cratons; (2) deposition of volcanogenic turbidites in either forearc or back-arc basin positions; (3) continued convergence of the cratons, and the formation of thrust sheets and horizontal folds along the northern margin of the South American craton; (4) erosion of these thrust sheets and primary deposition of the basal conglomerates and wackes; (5) sinistral shearing and felsic plutonism (Figure 5.2). Later, weathering of the orogenic rocks probably gave rise to the Rosebel Group.

This sequence is analogous to the proposed development of Paleoproterozoic rocks elsewhere in the Guiana shield, and also in other Paleoproterozoic circum-South Atlantic provinces in Brazil and in West Africa.

V. A. Guiana shield analogues and geochronology:

Rocks of the Paramaka, Armina, and Rosebel Groups are present in French Guiana, Guyana, and Venezuela (although the terminology is not always consistent). For purposes of this paper, analogous rocks in French Guiana are most relevant (in terms of local analogues). The Proterozoic rocks in French Guiana have been subject to numerous studies, so a great deal of data is available for comparison. The Ile de Cayenne and central Guiana complexes are two plutonic-volcanic complexes that are located in the northern, and central parts of French Guiana respectively. They are separated by the Orapu basin, and appear to converge in Suriname (Vanderhague et al., 1998). The

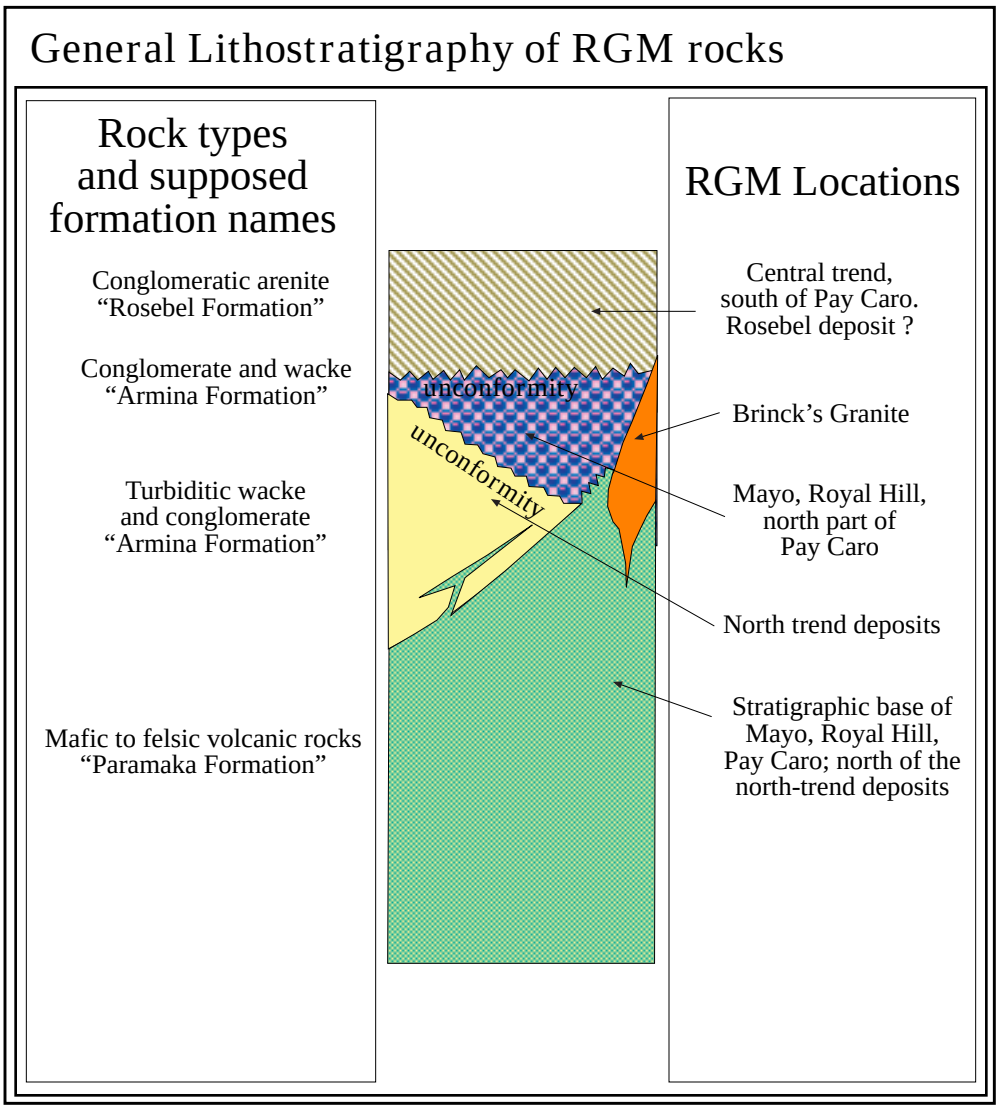

Figure 5.3: General lithostratographic column of the RGM concession. Rock types and the presently associated formation names are listed in the left column, and the deposits in which these rocks are found are listed in the right column. Modified from Vanderhage et al., (1998).

lithologies comprising the Ile de Cayenne complex and the central Guiana complex appear to have similar characteristics to those in Suriname.

Igneous rocks from the Paramaka Group, intermediate volcanic rocks, and granitic rocks are found in the Ile de Cayenne complex and the Central Guiana complex in French Guiana, as well as sedimentary rocks that comprise the Armina and Rosebel Groups in those locations. Metalavas and metatuffs comprising the Ile de Cayenne complex are considered by Vanderhague et al., (1998) to be part of the Paramaka Group. Vanderhague et al., (1998) also think that the sediments in the Orapu basin are thought to comprise the Armina Group, and the upper sedimentary formation (USU), which is equivalent to the Rosebel Group.

The Armina in French Guiana constitute flysch-like-sedimentary sequences characterized by folded rhythmic alternations of graded greywacke, sandstone, and tuff layers (Vanderhague et al., 1998). Some structural features of the Armina Group in the Orapu basin are similar to flyschoid rocks at RGM (mentioned above). The USU, thought to be an equivalent of the Rosebel Group at RGM is also present in the Orapu basin, and is described by Vanderhague et al., (1998) as being dominantly monomictic quartz-rich conglomerate and sandstone, with, in some cases, lenses of polymict conglomerate interpreted as debris flows. According to Vanderhague et al., (1998), the structural fabric of the USU is characterized by a steeply dipping foliation, S_2, in an axial plane position of meter to kilometer scale folds with horizontal to slightly plunging axes, and by a down-dip lineation L_2, marked by kyanite and white micas preferred orientation, and by stretched pebbles. This description of the USU is consistent, compositionally and structurally, with the rocks of the Pay Caro deposit at RGM.

Models of crustal evolution suggested by Vanderhague et al., (1998) concerning the rocks in the Ile de Cayenne complex and Central Guiana Complex, describe the early formation of tholeiitic-ocean crust, followed by the evolution of increasingly calk-alkaline-volcanic sequences. The late evolution of volcanic sequences and of the plutonic complexes suggests the formation of a magmatic source enriched in incompatible REE's, and the development of a thick crust generating highly potassic magmas and eventually peraluminous granite (Vanderhague et al., 1998). I propose the same argument is true for the evolution of the igneous rocks at RGM, as geochemical evidence paints a similar picture. Vanderhague et al., (1998) go on to back up this argument in French Guiana with U/Pb age-dating from zircons obtained from tholeiitic trondhjemite, tonalite, granite, and leucogranite from the central Guiana complex. Two trondhjemite samples yield the oldest ages of 2216 ± 4 Ma and 2174 ± 7 Ma, while tonalites yield younger ages of 2144 ± 6 Ma, 2129 ± 6 Ma, 2115 ± 7 Ma. Granite and leucogranite yield the youngest ages of 2094 ± 5 Ma, 2093 ± 8 Ma, and 2083 ± 8 Ma (Vanderhague et al., 1998). Preliminary U/Pb geochronology carried out at UNC on four zircons from tonalite to the south of the Royal Hill deposit indicates that they are approximately 2160 Ma. However, further geochronological work from the RGM rocks is necessary in backing up the previous argument.

V. B. Circum-South-Atlantic analogues:

The rocks described at RGM bear resemblance to other rocks in various terranes in the circum-south-Atlantic continents that were involved in the Transamazonian - Eburnean (in Africa) orogeny (Figure 5.4). Similar styles of sedimentation, structural evolution, and igneous evolution are recorded in the rocks of West Africa (associated

with the Mann and Congolese cratons), and in the rocks of the Saõ Fransiscan craton of Brazil.

The sedimentary rocks comprising what is considered to be the Armina Formation in Suriname and French Guiana have characteristics similar to the Birimian rocks of west Africa. The Boromo-Goren Greenstone belt (BGGB) of Burkina Faso forms part of the Paleoproterozoic Birimian domain of the West African Craton. The Goren segment of this greenstone belt trends SE across Burkina Faso for a distance of approximately 140km, and constitutes an arcuate extension to the predominantly northerly-trending, 500km long segment of the belt (Hein et al., 2003). According to Hein et al., (2003), two Birimian formations are described in the Goren segment: (1): a volcano-sedimentary package with intercalated fluvio-deltaic metasediments comprises the lower Birimian (mentioned above as an analogue to the north-trend sedimentary rocks) that are unconformably overlain by (2) a volcanic-volcaniclastic package comprising the upper Birimian. The Birimian formations were deformed during the Eburnean Orogeny at approximately 2.1 Ga, and intruded by numerous syn-to post tectonic granitoids.

The multiphase development of the Birimian terrane is described by Milési et al., (1992) as follows: (1) Deposition of sedimentary units associated with Dabakalian granite, coeval with volcanic and volcano-sedimentary rocks (pre-2150 Ma) to until B_1 (2150 – 2100 Ma). These rocks are mainly flyschoid, with tholeiitic volcanic rocks and volcano-sedimentary intercalations. The detritus of unit B_1 was derived mostly from Early Proterozoic (Dabakalian) rocks (Milési et al., 1992). (2) Pre-B_2 crustal thickening related to D_1 thrusting. (3) Deposition of unit B_2 comprising volcanic trough sequences

Circum-South Atlantic Paleoproterozoic Provinces

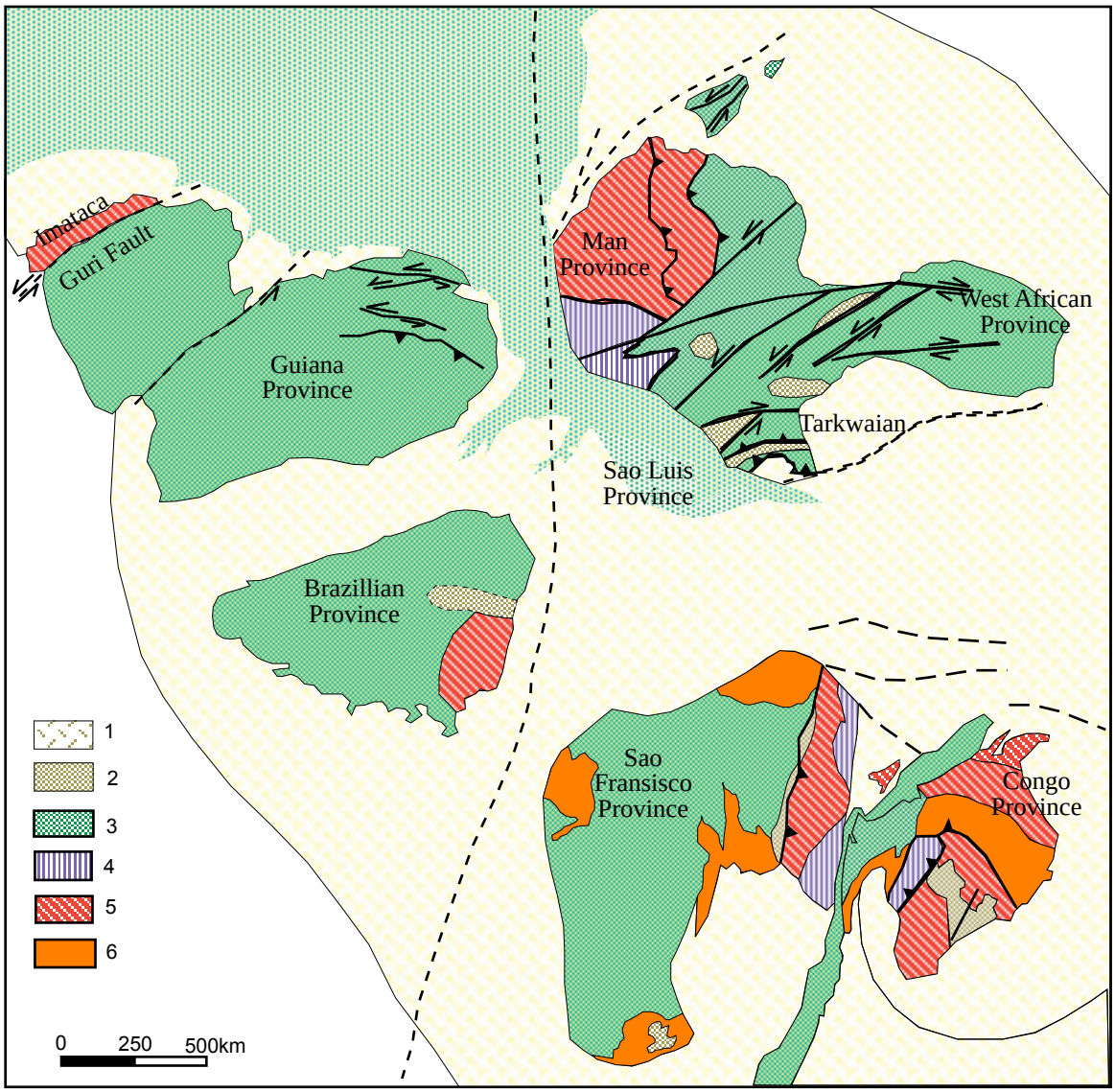

Figure 5.4: Schematic map of circum-South Atlantic Paleoproterozoic provinces. 1: Post-paleoproterozoic sediments; 2: fluvio-deltaic formations; 3: undifferentiated Paleoproterozoic; 4: high-grade Paleoproterozoic metamorphic rocks; 5: Archaean granulites; 6: Archaean granites and migmatites. Figure from Ledru et al., (1994).

of varying composition (tholeiitic with rare komatiitic intercalations, bimodal and tholeiitic to calc-alkaline, volcano-plutonic) and Tarkwaian clastic infill basin deposits.

Based on lithological, structural, petrological and geochemical data by Abouchami et al. (1990), Leube et al. (1990), Boher et al. (1992), Sylvester and Attoh (1992), Feybesse and Milesi (1994), Ama Salah et al. (1996), Hirdes et al. (1996), Pouclet et al. (1996), Doumbia et al. (1998), Hirdes and Davis (1998), John et al. (1999), and Béziat et al. (2000), the Paleoproterozoic Birimian greenstone belts of Baoulé-Mossi domain of West Africa were accreted between 2165 and 2085 Ma (Feybesse and Milési, 1994) onto Archaean continental crust (Hein et al., 2003).

Three conformable sedimentary successions are reported in the lower Birimian rocks by Hein et al., (2003), and are (1): volcaniclastic quartzite, tuffaceous metagraywacke, siltstone, and shale; (2): mafic-intermediate volcanic succession consisting of alternating units of massive basalt to andesite, intercalated with beds of breccia and tuff; (3) an upper volcano-sedimentary succession with thin beds of siltstone, shale, feldspathic quartzite, gravel to boulder sized conglomerate, and immature breccias and tuff. The first and third successions are turbiditic, and show parts of, if not complete Bouma sequences (Hein et al., 2003). These sedimentary rocks seem to have similar characteristics to some of the sediments at RGM, and probably represent the same sequence of island arc development, as do the rocks at RGM.

Similar styles of Paleoproterozoic volcanism are present in West Africa in the Guiana Shield. Rocks ranging in composition from Tholeiites to leucogranites are present in both regions, and probably reflect a similar sequence of events. Calc-alkaline igneous rocks are dated in Senegal at 2079±9 Ma (Pb/Pb on zircons) and in Mali at 2074

±7Ma (U/Pb on zircons, respectively, by Claves (In Milési et al., 1989) and Liegeois et al., (1991) (Marcoux and Milési, 1993). This seems to match up fairly well with 2094 ± 5 Ma, 2093 ± 8 Ma, and 2083 ± 8 Ma reported by Vanderhague et al (1998) for the calk-alkaline volcanism in French Guiana marking the latest stage of the Transamazonian orogeny in that location (Vanderhague et al., 1998).

Another probable analogue to the rocks at RGM is found in the Tarkwaian group of rocks in Burkina Faso. The Tarkwaian group in Burkina Faso lies unconformably on the Birimian formation (Gay, 1956, in Bossiere, 1996), and are composed of metapelite, metasandstone, and metaconglomerate. Sediments comprising the Tarkwaian rocks are composed of quartz, rhyolite, chert, schist, and mafic volcanic rocks (Bossiere et al., 1996). Bossiere et al., (1996) speculate that the Tarkwaian rocks were deposited in intramontaine basins, for example, grabens associated with rifting. The mixed clast population of fluvial detritus and volcaniclastic components is explained by Bossiere et al., (1996) as resulting from synchronous volcanism and terrigenous deposition in an intramontaine basin as mentioned above. Detrital zircon ages obtained from metaconglomerates from the Tarkwa are reported by Bossiere et al., (1996) at 2148 ± 4 MA, and 2145 ± 8 MA. The Tarkwa seems like a likely analogue to the rocks of Pay Caro that contain both terrigenous and volcanic clastic material.

VI. Conclusions:

The sedimentary rocks at RGM show four different lithofacies associations. (1) A deep-water, turbiditic series of wackes, conglomerates, and mudstones comprise the north-trend rocks. These rocks consist of distal to proximal facies and deposit mafic and felsic clastic material in a submarine slope environment. (2) Steep, syn-deformational sub-aerial to shallow-water alluvial processes disperse mafic and felsic sediment of the Royal Hill deposit. These deposits probably originated in an alluvial fan - braided stream environment. (3) Alluvial deposits in the Mayo area show bimodal volcanic association and are related to late-phase volcanism. (4) A shallow marine deposit in which volcanic and terrigenous material comprise proximal facies, and mainly terrigenous material comprises distal facies is evident in the rocks of Pay Caro. This sequence is unconformably overlain by a younger, mainly terrigenous conglomeratic sandstone, locally, the Rosebel Group.

Volcanic rocks of RGM reflect a changing island arc-system during the Paleoproterozoic. Royal Hill mafic volcanic rocks represent the earliest phase of volcanism, and are relatively un-enriched in incompatible REE's, although they are still 10 to 20 times more enriched in REE's than chondrites, and are therefore probably arc-basalts. Pay Caro rocks represent intermediate phase of volcanism, and have a greater enrichment in incompatible REE's. Finally, Mayo rocks the most enriched in incompatible REE's, and probably represent the most advanced phase of volcanism in the

life of the island arc system. Brinck's granite is similarly enriched in incompatible REE's as are the Mayo igneous rocks, and is therefore also associated with a later phase of magmatism than the other igneous rocks at RGM.

Structural evolution of the RGM rocks is polyphase, and probably represents three deformational events: (1) Early thrusting and nappe-folding related to the initial stages of the Transamazonian orogeny; (2) Refolding of early nappe-style folds, and development of a penetrative axial planar foliation; (3) Sinistral strike slip deformation related to the final stages of the Transamazonian orogeny.

The rocks at RGM have direct analogues throughout the Proterozoic in the rocks elsewhere in the Guiana shield. The Paramaka, Armina, and Rosebel Groups in French Guiana should not be discarded as relevant analogues. Although volcanism, and sedimentations vary through space and time so these rocks will have different characteristics in different locations, they should not be disregarded as useful references.

The rocks at RGM are analogous to a great number of Archaean and Proterozoic greenstone-belts described throughout the world. Examples from the Rio das Velhas greenstone belt in Brazil, the Birimian greenstone belts in west Africa, arc-related rocks in the Canadian shield, greenstone belts in India, and many other places are relevant analogues to the rocks at RGM.

Appendix I: Petrographic Data

Slide	Drillhole	Depth	Qm	F	Lt(fels)	Lt(maf)	Lt(sed)	Lt(Porph)	LT(Quartzite)	Matrix	F	Q	L	F	Qm	Lt	Lithology
20	MDH-140	123.8	3	4	19.5	5	0	50	0	19	3.5	3	94	4	3	93.5	Basal conglomerate
21	MDH-140	123.8	2	3	15.5	44.5	0	25	2.5	8	2.5	4.5	93	3	2	95.5	Basal conglomerate
23	MDH-140	60.6	1	7	8	33.5	0	36.5	0	14	7	1	92	7	1	92	Basal conglomerate
24	MDH-140	60.6	3	11	14.5	47.5	0	0.5	0.5	23	11	3.5	86	11	3	86	Basal conglomerate
25	MDH-140	60.6	4.5	8	7	18	0	8.5	11.5	43	7.5	16	77	8	4.5	88	Basal conglomerate
26	MDH-141	82.08	0	4	13.5	39	0	27	0.5	16.5	3.5	0.5	96	4	0	96.5	Basal conglomerate
27	MDH-141	82.08	0.5	3	5.5	22	0	38.5	11	19	3	12	85	3	0.5	96	Basal conglomerate
28	MDH-141	82.08	0	9	7	19	0	34	7	24	9	7	84	9	0	91	Basal conglomerate
29	MDH-141	82.08	0.5	8	29	30	0	11	2	19.5	8	2.5	90	8	0.5	91.5	Basal conglomerate
30	PC-111	113	0	6	23	32.5	0	0	33.5	0	6	34	56	6	0	89	Basal conglomerate
31	PC-111	113	2	1	6	54.5	0	0	37	0	0.5	39	61	1	2	97.5	Basal conglomerate
32	PC-111	113	0	0	27.5	49.5	0	0	23	0	0	23	77	0	0	100	Basal conglomerate
33	PC-111	113	3	0	8	69	0	0	20	0	0	23	77	0	3	97	Basal conglomerate
34	PC-64	186.2	0.5	0	28.5	66	0	3.5	1.5	0	0	2	98	0	0.5	99.5	Basal conglomerate
35	RHD-135	128.6	5	5	11.5	26.5	0	0	38.5	14	4.5	44	52	5	5	90.5	Basal conglomerate
36	RHD-135	128.6	0.5	0	0	1.5	0	0	94.5	3.5	0	95	5	0	0.5	99.5	Basal conglomerate
37	RHD-135	128.6	0	0	0	97.5	0	0	2.5	0	0	2.5	98	0	0	100	Basal conglomerate
38	RHD-135	128.6	4.5	5	23.5	27.5	0	0	32.5	7.5	4.5	37	59	5	4.5	91	Basal conglomerate
39	RHD-135	128.6	7	4	10	49.5	0	0	16.5	13	4	24	73	4	7	89	Basal conglomerate
40	RHD-135	128.6	4	1	41	51	0	0	0	3	1	4	95	1	4	95	Basal conglomerate
41	RHD-135	128.6	4.5	0	6.5	4.5	0	9	59	16.5	0	64	37	0	4.5	95.5	Basal conglomerate
42	RHD-135	128.6	7	3	8	0	24	19	5.5	34	2.5	13	85	3	7	90.5	Basal conglomerate
43	RHD-114	95.5	2.5	3	37.5	30.5	0	0	14	12.5	3	17	81	3	2.5	94.5	Conglomeratic wacke
44	RHD-114	95.5	2.5	8	21.5	23.5	0	0	21.5	23	8	24	68	8	2.5	89.5	Conglomeratic wacke
45	RHD-114	95.5	6	5	27	9.5	0	0	13.5	39.5	4.5	20	76	5	6	89.5	Conglomeratic wacke
46	RHD-123	98.25	0.5	1	2.5	0	0	31	46.5	18.5	1	47	52	1	0.5	98.5	Basal conglomerate
47	SP-05	64	0.5	0	17	0	0	63	1.5	18	0	2	98	0	0.5	99.5	Conglomeratic wacke
48	SP-05	64	2	3	18	6	0	32	6	33.5	2.5	8	90	3	2	95.5	Conglomeratic wacke
49	SP-05	64	1	0	31.5	5.5	0	35.5	2	24.5	0	3	97	0	1	99	Conglomeratic wacke
50	SP-05	64	1.5	1	0	1	25	56.5	1	14.5	0.5	2.5	97	1	1.5	98	Conglomeratic wacke
51	SP-05	64	0	2	0	42.5	9.5	35.5	0.5	10.5	1.5	0.5	98	2	0	98.5	Conglomeratic wacke
52	SP-05	64	0.5	2	0	0	6	58	4	30	1.5	4.5	94	2	0.5	98	Conglomeratic wacke
53	JZ-59	92.65	3	5	3.5	0	8	45.5	3.5	31.5	5	6.5	89	5	3	92	Conglomeratic wacke
54	JZ-59	92.65	1.5	2	9	24.5	0	45	0	18.5	1.5	1.5	97	2	1.5	97	Conglomeratic wacke
55	JZ-59	92.65	6	1	24.5	0	0	22.5	7.5	39	0.5	14	86	1	6	93.5	Conglomeratic wacke
56	JZ-59	92.65	22.5	12	2	4	0	0	13	47	12	36	53	12	23	66	Conglomeratic wacke
57	JZ-59	97.7	4.5	0	27.5	13	0	8	23	24	0	28	73	0	4.5	95.5	Conglomeratic wacke
58	JZ-59	97.7	3.5	0	31	37.5	0	10	2.5	15.5	0	6	94	0	3.5	96.5	Conglomeratic wacke
59	JZ-59	97.7	5.5	0	14.5	45	0	0	11.5	23.5	0	17	83	0	5.5	94.5	Matrix supported conglomerate
60	KH-84	105.2	3	11	3.5	24	0	23.5	13	22.5	11	16	74	11	3	86.5	Matrix supported conglomerate
61	KH-84	105.2	0.5	2	0	2.5	0	87.5	4.5	3.5	1.5	5	94	2	0.5	98	Matrix supported conglomerate

62	KH-84	105.2	13	6	17	5	0	34.5	7	18	5.5	20	75	6	13	81.5	Matrix supported conglomerate
63	KH-84	105.2	8	6	10	6.5	0	33.5	5	31.5	5.5	13	82	6	8	86.5	Matrix supported conglomerate
64	JZ-59	90.6	12.5	13	6.5	0	0	19.5	7.5	41	13	20	67	13	13	74.5	Matrix supported conglomerate
65	JZ-59	90.6	11	11	6	0	0	33	7	32.5	11	18	72	11	11	78.5	Matrix supported conglomerate
66	JZ-74	131.6	4.5	8	27.5	23.5	0	9	9	18.5	8	14	79	8	4.5	87.5	Matrix supported conglomerate
67	JZ-74	131.6	11.6	5	6.5	0	0	38.5	7.5	31.5	4.5	19	77	5	12	84	Matrix supported conglomerate
68	TP-20	19.1	8	29	0.5	0	19	0	3.5	40	29	12	60	29	8	63	Matrix supported conglomerate
69	TP-20	19.1	6	31	0	0	30	0	0	33.5	31	6	64	31	6	63.5	Matrix supported conglomerate
70	TP-20	19.1	0	26	0	0	17	0	6	51.5	26	6	69	26	0	74.5	Matrix supported conglomerate
71	TP-20	19.1	5.5	39	0	0	0	0	2.5	53.5	39	8	54	39	5.5	56	Conglomeratic wacke
72	PC-67	139.6	7.5	2	9	5.5	0	0	34.5	41.5	2	42	56	2	7.5	90.5	Pebble conglomerate
73	PC-67	139.6	13.5	1	8.5	4.5	0	0	32.5	40.5	0.5	46	54	1	14	86	Pebble conglomerate
74	PC-67	139.6	12	0	27	16	0	0	25	20	0	37	63	0	12	88	Pebble conglomerate
75	PC-67	139.6	14	1	20	16	0	0	28	21	1	42	57	1	14	85	Pebble conglomerate
76	PC-230	160	6.5	7	20	19	0	0	27.5	10	7	34	49	7	6.5	76.5	Pebble conglomerate
77	PC-230	160	2	0	21	18	0	5.5	43	10.5	0	45	55	0	2	98	Pebble conglomerate
78	PC-230	160	2	0	21.5	9	0	17	24.5	26	0	27	74	0	2	98	Pebble conglomerate
79	PC-64	132.5	1	1	46.5	7.5	0	0	32	12.5	0.5	33	67	1	1	98.5	Pebble conglomerate
80	PC-64	132.5	10	1	32	13.5	0	0	17	27	0.5	27	73	1	10	89.5	Pebble conglomerate
81	RHD-135	95.5	4.5	28	11	4	0	0	8	44.5	28	13	60	28	4.5	67.5	Conglomeratic wacke
82	RHD-135	95.5	2	19	28.5	7	0	13.5	8.5	21.5	19	11	71	19	2	79	Conglomeratic wacke
83	RHD-135	95.5	10	30	4	3.5	0	0	14	39	30	24	47	30	10	60.5	Conglomeratic wacke
84	RBD-67	114	19	28	5.5	0	0	0	32	15.5	28	51	21	28	19	53	Conglomeratic wacke
85	RBD-67	113.9	23	31	0	0	0	0	23	23	31	46	23	31	23	46	Conglomeratic wacke
86	RBD-67	113.9	315	18	2	0	0	0	37	11.5	18	352	14	18	315	50.5	Conglomeratic wacke
87	RBD-67	113.9	18.5	27	0	12	0	0	34	9	27	53	21	27	19	55	Conglomeratic wacke
88	MDH-141	94.5	10	30	0	0.5	0	0	5	54.5	30	15	55	30	10	60	Wacke
89	MDH-141	94.5	11.5	39	0	0	0	0	1.5	48.5	39	13	49	39	12	50	Wacke
90	MDH-141	94.5	14.5	39	0.5	0	0	0	0	46.5	39	15	47	39	15	47	Wacke
91	MDH-141	94.5	16	43	0	0	0	0	0.5	40.5	43	17	41	43	16	41	Wacke
101	PC-458	153.8	30	1	0	0	0	0	23	46	1	53	46	1	30	69	Wacke
102	PC-411	69	7.5	1	0	0	0	0	78	14	0.5	86	14	1	7.5	92	Wacke
103	PC-404		8	1	0	0	0	0	79	12	1	87	12	1	8	91	Conglomeratic wacke
104	PC-411	12.5	0	0	0	0	0	0	72.5	15	0	15	15	0	0	87.5	Conglomeratic wacke
105	PC-404		18.5	2	0	0	0	0	61	18.5	2	37	19	2	19	79.5	Conglomeratic wacke
106	PC-411	69	12.5	0	11.5	0	0	0	42.5	33.5	0		45	0	13	87.5	Conglomeratic wacke

Appendix II: Geochemical Data

Drill hole	Depth(m)	Rock type	TiO2	Zr	Y	Ce	Dy	Er	Eu	Gd	Ho	La	Lu	Nb	Nd	Pr	Rb	Sm	Ta	Tb	Th	Tl	Tm	Yb
JZ-047	122.2	Felsic volc.	0.46	141	14.5	29.2	2.85	1.7	0.94	2.95	0.56	14.7	0.24	5.1	13.5	3.48	27.2	2.67	0.5	0.47	1.94	-0.5	0.24	1.5
JZ-047	135.2	Felsic volc.	0.41	113	15.2	29.3	2.52	1.49	0.82	2.63	0.5	14.4	0.22	5	12.6	3.1	27.9	2.55	0.4	0.44	1.65	-0.5	0.21	1.41
JZ-091	71.6	Int. volc.	0.71	92	23.2	21.2	4.01	2.65	1.02	3.56	0.89	9.7	0.39	3.9	11.3	2.72	10.1	2.87	0.3	0.59	1.02	-0.5	0.38	2.51
JZ-091	102	Int. volc.	0.75	92	19.4	20.2	3.45	2.14	0.9	3.17	0.71	9	0.34	4.1	11	2.64	42.8	2.73	0.3	0.52	1.01	-0.5	0.32	2.14
JZ-091	123	Int. volc.	0.75	92	18.5	18.6	3.31	2.19	0.89	3.01	0.73	8.4	0.34	4	10.3	2.43	1.3	2.53	0.3	0.51	0.97	-0.5	0.32	2.11
JZ-091	177.2	Int. volc.	0.66	97	16.5	21.2	3.06	2	0.95	2.95	0.67	10.2	0.31	4	10.9	2.69	18.7	2.61	0.3	0.51	1.13	-0.5	0.29	1.96
JZ-089	75	Int. volc.	0.66	114	17.5	25.4	2.8	1.91	0.88	2.77	0.61	12	0.3	6.4	11.9	2.8	26.5	2.55	0.5	0.49	1.84	-0.5	0.29	1.89
JZ-089	102	Int. volc.	0.65	115	19.5	28.6	3.11	1.97	0.95	3.15	0.66	13.3	0.31	6.3	13.5	3.13	19.5	3.02	0.5	0.51	1.95	-0.5	0.3	1.88
JZ-089	150	Int. volc.	0.5	117	14.8	27.4	2.81	1.82	0.82	2.8	0.59	13.3	0.28	5.7	11.9	2.91	14.7	2.63	0.5	0.45	2.35	-0.5	0.29	1.82
JZ-089	175.8	Int. volc.	0.84	118	20.7	21.7	3.8	2.37	1.02	3.37	0.84	10.6	0.38	6	11.4	2.74	27.1	2.61	0.4	0.62	1.07	-0.5	0.36	2.51
JZ-089	196.5	Int. volc.	0.74	90	18.4	16.6	3.29	2.02	0.89	2.77	0.75	7.4	0.37	4.2	9	2.09	4	2.28	0.3	0.5	0.86	-0.5	0.34	2.25
JZ-090	102	Int. volc.	0.63	114	16.5	23.3	2.8	1.82	0.85	2.58	0.6	11.3	0.27	4.1	11.5	2.87	1.5	2.62	0.4	0.47	1.85	-0.5	0.26	1.71
JZ-090	124.5	Int. volc.	0.71	131	18.7	26.5	3.17	2.03	0.92	2.99	0.68	13.1	0.31	4.6	13	3.24	0.4	2.92	0.4	0.51	1.94	-0.5	0.31	1.98
JZ-090	148.2	Int. volc.	0.63	113	16.3	23	2.93	1.8	0.87	2.77	0.63	11.2	0.29	4.1	11.1	2.75	5.1	2.58	0.4	0.49	1.61	-0.5	0.28	1.74
RMD 027	99.6	Felsic tuff	0.44	315	22.7	76.8	3.77	2.34	1	4.57	0.8	41.4	0.36	10.7	30	8.33	101.5	5.34	0.9	0.64	21.8	-0.5	0.35	2.36
RMD 027	125.2	Felsic tuff	0.39	269	17.5	72.4	3.05	1.92	0.92	4.31	0.62	39.1	0.27	9.2	28.3	7.93	118	4.85	0.8	0.56	18.3	0.5	0.27	1.85
RMD 027	149.6	Felsic tuff	0.37	-2	-0.5	-0.5	-0.05	-0.03	-0.03	-0.05	0.01	-0.5	0.01	-0.2	-0.1	-0.03	-0.2	-0.03	0.2	-0.01	-0.05	-0.5	0.01	-0.03
RMD 028	75	Felsic tuff	0.4	283	20.4	73.5	3.76	2.23	1.08	4.82	0.77	39.3	0.35	10.5	28.1	7.84	127	4.74	0.8	0.67	19.9	-0.5	0.34	2.26
MHD 133	149.7	Int. tuff	0.51	90	15	19.6	2.64	1.58	0.86	2.71	0.6	8.8	0.26	3.8	10.6	2.49	20.2	2.3	0.2	0.45	1.14	-0.5	0.24	1.6
MHD 134	84	Int. volc.	1.26	129	26.1	94	5.94	2.86	3.32	9.78	1.08	37.7	0.36	6.5	56.8	13.5	14.7	10.55	0.4	1.28	1.98	-0.5	0.39	2.51
MHD 134	103.5	Mafic volc.	1.16	121	23.8	72.6	5.37	2.52	3.46	8.05	1	28.5	0.33	6	43.6	10.1	6.6	8.36	0.3	1.05	1.73	-0.5	0.36	2.18
RMD 014	102	Felsic tuff	0.4	293	20.2	82.7	3.43	2.06	0.98	4.41	0.72	44.1	0.32	10.6	31.6	8.78	127.5	5.39	0.8	0.63	19.7	0.5	0.31	2.09
RMD 014	124.8	Felsic tuff	0.41	294	19.7	80.1	3.31	2.04	0.97	4.28	0.7	42.9	0.32	10.5	30.4	8.54	132	5.24	0.8	0.61	19.5	0.5	0.31	2.06
RMD 014	144.5	Felsic tuff	0.4	279	19.3	75	3.43	2.01	1	4.43	0.69	40.5	0.29	10.4	28.7	7.98	141	4.9	0.7	0.61	18.4	0.5	0.31	2.1
RMD 026	105	Felsic tuff	0.13	153	21.5	50.7	3.66	2.52	1.14	4	0.83	22.8	0.45	5.8	21.1	5.94	32	3.81	0.5	0.61	3	-0.5	0.4	2.62
RMD 026	126	Felsic tuff	0.13	151	21.1	53.9	3.75	2.41	1.19	4.22	0.83	25.3	0.44	6.5	23.4	6.58	22.4	4.11	0.5	0.66	2.99	-0.5	0.39	2.52
RMD 026	147.3	Felsic tuff	0.13	154	21.7	53.2	3.73	2.53	1.19	4.11	0.84	24.6	0.46	6.4	23	6.43	31.8	3.9	0.5	0.66	2.95	-0.5	0.41	2.78
PC 375	101.2	Int. volc.	1.02	109	21.8	33.1	4.21	2.51	1.42	4.27	0.93	14.3	0.4	7.3	17.9	4.42	9.7	4.01	0.5	0.73	1.09	-0.5	0.39	2.37
PC 375	128.3	Int. volc.	0.61	109	15.9	24.8	2.88	1.83	0.87	2.8	0.66	11.6	0.32	4.9	11.7	3.05	4.4	2.56	0.4	0.51	1.56	-0.5	0.3	1.86
PC 375	149.3	Int. volc.	0.74	132	20.6	30.8	3.81	2.34	1.15	3.73	0.85	14.4	0.38	6.5	14.5	3.83	1.7	3.25	0.5	0.64	2.01	-0.5	0.37	2.33
PC 350	130	Mafic volc.	0.79	100	21	22	3.92	2.46	0.98	3.35	0.85	9.5	0.39	5.7	11.4	2.87	18.1	2.76	0.4	0.61	0.84	-0.5	0.36	2.36
PC 350	147.9	Mafic volc.	0.78	68	16.4	16.4	2.97	1.99	0.93	2.72	0.66	7.2	0.31	4	9.2	2.2	7.1	2.35	0.3	0.53	0.66	-0.5	0.31	1.88
PC 350	176.2	Int. volc.	0.62	107	16.9	22.4	3	1.93	0.83	2.73	0.68	10.2	0.31	4.5	10.4	2.68	19.1	2.47	0.4	0.49	1.47	-0.5	0.3	1.97
PC 350	200.7	Int. volc.	0.62	107	17	23.4	3.13	1.96	1	2.98	0.68	10.9	0.32	4.7	10.9	2.89	30	2.45	0.4	0.52	1.52	-0.5	0.31	1.87
PC 350	223.9	Mafic volc.	0.68	123	18.4	25.5	3.28	2.09	0.99	3.04	0.74	11.9	0.34	5.2	12.2	3.14	2.8	2.7	0.4	0.53	1.66	-0.5	0.33	2.06
PC 350	249.6	Mafic volc.	0.65	117	18	22.9	3.35	2.11	0.97	3	0.73	10.6	0.33	5.1	10.7	2.83	33.4	2.35	0.4	0.53	1.62	-0.5	0.33	2.08
PC-415	257.5	Int. volc.	0.82	141	21.3	50.3	4.26	2.55	1.33	4.68	0.87	24.8	0.39	7.6	22.2	6.11	115	4.37	0.6	0.74	7.59	-0.5	0.4	2.39
PC-415	280	Int. volc.	0.82	180	22.6	59.9	4.29	2.67	1.29	4.88	0.96	29.2	0.41	9.7	24	6.74	116	4.57	0.8	0.77	10.2	-0.5	0.39	2.49
PC-415	298.7	Int. volc.	0.77	124	15.8	50.7	3.26	1.85	1.3	3.92	0.68	22.2	0.31	6.6	21	5.73	81	4.1	0.5	0.58	4.61	-0.5	0.29	1.76
RHD 587	150	Mafic volc.	0.78	45	13.8	6.7	2.56	1.56	0.66	2.16	0.55	2.5	0.21	2	5.1	1	3.7	1.64	0.1	0.39	0.22	-0.5	0.22	1.47
RHD 587	168.9	Mafic volc.	0.82	49	15.1	7	2.72	1.68	0.68	2.21	0.6	2.7	0.25	2	5.2	1.04	4.4	1.75	0.1	0.43	0.24	-0.5	0.23	1.67

RHD-478	102.7	Mafic volc.	1.1	57	18.5	10.6	3.61	2.2	0.97	3.09	0.8	4.1	0.33	3.1	7.7	1.63	2.7	2.37	0.2	0.59	0.35	-0.5	0.35	2.07
RHD-478	124	Mafic volc.	1.65	102	29.3	15.8	5.57	3.56	1.42	4.65	1.24	5.8	0.56	5.3	11.8	2.46	22.1	3.65	0.4	0.91	0.62	-0.5	0.55	3.27
RHD-478	148.6	Mafic volc.	0.85	50	15	8	2.7	1.67	0.67	2.16	0.58	3.1	0.24	2.4	5.7	1.18	2.1	1.73	0.2	0.43	0.28	-0.5	0.24	1.58
RHD-478	175	Mafic volc.	0.82	50	15.1	8.3	2.78	1.68	0.72	2.21	0.59	3.4	0.23	2.4	6	1.21	3.2	1.83	0.2	0.45	0.28	-0.5	0.23	1.62
RHD-478	201.8	Mafic volc.	1.24	69	21.9	11.7	3.85	2.52	1.03	3.1	0.88	4.4	0.34	3.6	8.6	1.72	4.9	2.56	0.2	0.62	0.38	-0.5	0.36	2.35
MDH-150	125	Felsic volc.	0.12	155	23.2	54.5	3.64	2.54	1.11	4.14	0.8	25.9	0.41	6.1	24.5	6.5	22.2	4.48	0.5	0.62	2.98	-0.5	0.38	2.61
MDH-135	143.2	Felsic volc.	0.54	50	11.5	11.1	2.01	1.34	0.52	1.84	0.45	5.5	0.2	2.1	6.5	1.47	3.5	1.69	0.1	0.35	0.54	-0.5	0.19	1.22
RMD-24	102.35	Felsic volc.	0.16	204	21.6	57.2	3.51	2.38	1.22	4.2	0.76	27.8	0.41	5.7	25.8	6.86	30.6	4.56	0.5	0.6	2.87	-0.5	0.35	2.52
RHD-116	139	Felsic volc.	0.87	52	16.4	7.5	2.91	1.9	0.71	2.12	0.65	3.2	0.28	2	5.9	1.12	12.4	2.06	0.1	0.44	0.25	-0.5	0.27	1.78
PC-20	76	Int. volc.	1.05	146	26.2	31.2	4.3	2.69	1.15	3.97	0.89	13.7	0.41	7.1	17.2	3.96	0.3	3.92	0.5	0.65	1.07	-0.5	0.4	2.68
RMD-22	64.7	Felsic volc.	0.14	166	20	50.2	3.15	2.1	0.89	3.42	0.68	24.4	0.37	6.5	22.4	5.99	23.3	3.97	0.5	0.48	2.83	-0.5	0.32	2.24

Works Cited

Attoh, K. and Ekwueme, B.N., The West African Shield. 1997, in De Wit, M.J., and Ashwal, L.D. Greenstone Belts, (editors). Oxford monographs on Geology and Geophysics 35 (1997). Clarendon Press, Oxford. pp. 91 - 124.

Baltazar, O.F., Zucchetti, M., 2007. Lithofacies associations and structural evolution of the Archaean Rio das Velhas greenstone belt, Quadrilatero Ferrifero, Brazil: A review of the setting og gold deposits. Ore Geology Reviews (2007), doi:10.1016/j.oregeorev.2005.03.021

Barrett, T.J., Maclean, W.H. 1993. Lithogeochemical techniques using immobile elements. Journal of Geochemical exploration, 48 (1993) 109 - 133. Elsevier Science Publishers B.V., Amsterdam

Boggs, S. Jr. 2001. Principles of Sedimentology and Stratigraphy. Prentice Hall, Inc. Upper Saddle River, NJ 07458. 726 p.

Bosma, W., Groeneweg, W., (1969), Review of the stratigraphy of Suriname. Geologie en Mijnbouw Dienst, 1969, 4; 31 pp.

Bosma, W., Kroonenberg, S.B., Mass, K., De Roever, E.W.F., 1983. Igneous and metamorphic complexes of the Guiana Shield in Suriname. Geologie en Mijnbouw 62, 241-254 (in Gibbs and Barron, 1993)

Bossière, G., Bonkoungou, I., Peucat, J.P., 1996. Origin and age of Paleoproterozoic conglomerates and sandstones of the Tarkwaian Group in Burkina Faso, West Africa. Precambrian Research 80 (1996) 153 - 172

Brinck, J.W. 1955. Goudafzettingen in Suriname (Gold deposits in Surinam, with an English Summary). Unpublished Ph.D. dissertation. Rijksuniversiteit of Leiden, Netherlands. 1955. 246 pp.

Cambior Inc. 2003. Gross Rosebel Deposit feasibility report. Unpublished. 125pp.

Delor, C., Lahondére, D., Egal, E., Lafon, J.M., Coucherie, A., Guerrot, C., Rossi, P., Truffert, C., Théveniaut, H., Phillips, D., Avelar, V.G. 2003. Transamazonian Crustal Growth and Reworking as revealed by the 1:500,000-scale Geological map of French Guiana (2nd edition). Géologie de la France, 2003. # 2-3-4, P. 5-57.

Dickinson, W.R., Beard, L.S., Brakenridge, G.R., Erijavec, J.L. , Ferguson, R.C., Inman, K.F., Knepp, R.A., Lindberg, F.A., Ryberg, P.T. 1983. Provenance of North American Phanerozoic sandstones in relation to tectonic setting. Geological Society of America Bulletin, v. 94, p. 222 - 235

Eriksson, K.A., Krapez, B., Fralick, P.W. Sedimentological Aspects. 1997. in De Wit, M.J., and Ashwal, L.D., Greenstone Belts, (editors) Oxford monographs on Geology and Geophysics 35 (1997). Clarendon Press, Oxford. pp. 91 - 124.

Eriksson, K.A., Krapez, B., Fralick, P.W., 1994. Sedimentology of Archaean greenstone belts: signatures of tectonic evolution. Earth Science Reviews 37 (1994) 1 - 88

Folk, R.L., 1974. Petrology of Sedimentary Rocks. Hemphill, Austin, TX, 182 p.

Gibbs, A. K., Barron, C. N., 1993. The Geology of the Guiana Shield. Oxford Monographs on Geology and Geophysics. 213 pp.

Gibbs, A.K., Barron, C.N., 1993. Geology of the Guiana Shield. Oxford monographs on Geology and Geophysics, vol. 22. Clarendon Press, Oxford, 246 pp.

Hawkesworth, C.J., Gallagher, K., McDermott, F., Hergt, J.M., McDermott, F. 1993. Mantle and Slab Contributions in Arc Magmas. Annual Reviews of Earth and Planetary Science. 1993, 21:175 - 204

Hein, K. A.A., Morel, V., Kagonè, O., Kiemde, F., Mayes, K., 2004 Birimian lithological succession and structural evolution in the Goren segment of the Boromo-Goren Greenstone belt, Burkina Faso. Journal of African Earth Sciences 39 (2004) 1 - 23

Ijzerman, R. 1931. Outline of the Geology and Petrology of Suriname. Martinus Nijhof. The Hague, Netherlands. 1931. 519 pp.

Kusky, T.M., Vearncombe, J.R., Structural aspects of Greenstone Belts. 1997. in De Wit, M.J., and Ashwal, L.D., Greenstone Belts, (editors) Oxford monographs on Geology and Geophysics 35 (1997). Clarendon Press, Oxford. pp. 91 - 124.

Ledru, P., Johan, V., Milési J.P., Tegyey, M. 1994. Markers of the last stages of Paleoproterozoic collision: evidence for a 2 Ga continent involving circum- South Atlantic provinces. Precambrian Research. 69 (1994): 169 – 191

Marcoux, E., Milèsi, J.P., 1993 Lead isotope signature of Early Proterozoic Ore Deposits in Western Africa: Comparison with Gold Deposits in French Guiana. Economic Geology 88 (1993). 1862 - 1879

Sylvester, P.J., Archaean Granite Plutons. 1994. in Condie, K.C., Archaean Crustal Evolution (editor). 1994. Developments in Precambrian Geology 11. Elsevier Science B.V. (1994). p. 261 - 314.

Vanderhague, O., Ledru, P., Thièblemont, D., Egal, E., Cocherie, A,. Tegyey, M., Milèsi, J.P. Contrasting mechanisms of crustal growth - Geodynamic evolution of the Paleoproterozoic granite-greenstone belts of French Guiana. Precambrian Research. 92 (1998): 165 - 193

Voicu, G., Bardoux, M., Stevenson, R., 2001. Lithostratigraphy, geochronology, gold metallogeny in the northern Guiana Shield, South America: a review. Ore Geology Reviews 18 (2001) 211-236

Wang, Z., Wilde, S. A., Wang, K., Yu, L. A MORB-arc basalt-adakite association of the 2.5 Ga Wutai greenstone belt: late Archaean magmatism and crustal growth in the North China Craton. Precambrian Research, 131. (2004). 323 - 343.

Whalen, J.B., Currie, K. L., Chapell, B. W. 1987. A-type granites: geochemical characteristics, discrimination and petrogenesis. Contributions to mineralogy and petrology (1987). 95. 407 - 419

Wood, D.A. 1980. The Application of a Th-Hf-Ta Diagram to problems of Tectonimagmatic Classification and to Establishing the Nature of Crustal Contamination of Basaltic Lavas of the British Tertiary Volcanic Province. Earth and Planetary Science Letters, 50. (1980). 11 - 30

Wood, D.A., Joron, J.L., Treuil, M., A Re-appraisal of the use of Trace Elements to classify and discriminate between magma series erupted in different tectonic settings. Earth and Planetary Science Letters, 45. (1979). 326 - 336

Woodhead, J., Eggins, S., Gamble, J. 1993. High field strength and transition element systematics in island and back-arc basin basalts: evidence for multi-phase melt extraction and a depleted mantle wedge. Earth and PLanetary Science Letters, 114 (1993). 491 - 504. Elsevier Science Publishers B.V., Amsterdam